
Fast Magnetic Field Line Reconnection

A. M. Soward and E. R. Priest

Phil. Trans. R. Soc. Lond. A 1977 **284**, 369-417

doi: 10.1098/rsta.1977.0013

Email alerting service

Receive free email alerts when new articles cite this article - sign up in the box at the top right-hand corner of the article or click [here](#)

FAST MAGNETIC FIELD LINE RECONNECTION

BY A. M. SOWARD

School of Mathematics, University of Newcastle upon Tyne

AND E. R. PRIEST

*Department of Applied Mathematics, The University of St Andrews,
St Andrews, Fife, Scotland**(Communicated by K. Stewartson, F.R.S. – Received 10 November 1975)*

CONTENTS

	PAGE
1. INTRODUCTION	370
2. THE MATHEMATICAL PROBLEM	377
3. THE SIMILARITY SOLUTION	381
(<i>a</i>) The equations	382
(<i>b</i>) Lowest order outer solution	382
(<i>c</i>) Inner region equations	383
(<i>d</i>) Lowest order inner solution	384
(<i>e</i>) Higher order inner and outer solutions in region I	385
(<i>f</i>) Matching of inner and outer solutions	386
(<i>g</i>) Summary	386
(<i>h</i>) Petschek's solution	387
4. COMPLEX POTENTIALS FOR REGION I	388
5. THE SOLUTION FOR REGION II	392
6. THE ROTATIONAL SOLUTION FOR REGION I	394
7. THE ALFVÉN LAYER	399
8. THE ALFVÉN BOUNDARY LAYERS AND CENTRAL DIFFUSION REGION	402
9. AN INTEGRAL CONSTRAINT	406
10. DISCUSSION	408
APPENDIX A	412
APPENDIX B	416
REFERENCES	417

Petschek (1964) has given a qualitative model for fast magnetic field line reconnection, at speeds up to a significant fraction of the Alfvén speed. It is supposed that an electrically conducting fluid is permeated by an almost uniform magnetic field which reverses direction across a plane of symmetry parallel to the field lines. An almost uniform stream flows steadily towards the plane of symmetry and is maintained by pressure forces. Magnetic field line reconnection occurs at the origin inside a small central diffusion region. The reconnected magnetic field is swept away rapidly in two thin jets

aligned with the plane of symmetry. The inflow and outflow regions are separated by discontinuities at which the tangential components of the magnetic field and fluid velocity suffer abrupt changes.

Sonnerup (1970) and Yeh & Axford (1970), on the other hand, have given alternative solutions for the incompressible case which include a second set of discontinuities. Their solutions are of similarity type, valid over some length scale which is much less than the overall distance between the magnetic field sources but is much greater than the size of the central diffusion region. The second set of discontinuities is, however, unacceptable for an astrophysical plasma, since they need to be generated at corners in the flow rather than at the central diffusion region.

This paper presents other solutions for the incompressible case, which are locally self-similar, without discontinuities or singular behaviour at a second set of discontinuities. The solutions are valid everywhere outside the central diffusion region when the inflow Alfvén Mach number M_1 (see (2.3) below) is much less than unity and are valid at large distances from the diffusion region when $M_1 = O(1)$. The analysis has been summarized by Priest & Soward (1976). It puts Petschek's mechanism on a sound mathematical basis and shows that the discontinuities are not in general straight but curve away from the incoming flows. Our estimate of the maximum reconnection rate $M_{e, \max}$ (see (10.9) below) depends weakly on the value of the magnetic Reynolds number $R_{m, e}$ (see (10.7) below). It decreases from 0.2 when $R_{m, e} = 10$ to 0.03 when $R_{m, e} = 10^6$.

1. INTRODUCTION

When two regions of uniform magnetic field B_1 , equal in magnitude but opposite in direction, are placed in contact a current sheet is formed at the interface between the two regions. If the magnetic field permeates a stationary fluid of finite electrical conductivity the current sheet thickens and magnetic field is annihilated in a region of ever increasing width $l = \sqrt{(t^*/\mu\sigma)}$, where t^* is the time, μ is the magnetic permeability and σ is the electrical conductivity. By this process magnetic energy is degraded into heat through the ohmic dissipation j^{*2}/σ , where j^* is the electric current. Since the electric current is of order $B_1/(\mu l)$, the total ohmic dissipation per unit length of current sheet is of order $B_1^2/(\mu^2\sigma l)$, a quantity which evidently decreases as time proceeds.

A high dissipation rate can be maintained if there is fluid motion towards the plane of symmetry. In this case convection of the magnetic field lines can balance the competing effect of lateral diffusion. A simple dynamical model which isolates the effect has been investigated by Parker (1973*a*) and Priest & Sonnerup (1975). Consider the two-dimensional steady motion of a fluid with constant density ρ , which is referred to rectangular cartesian coordinates x^* , y^* . Suppose that the flow is potential and has velocity $\mathbf{u}^* = (U_1 x^*/l, -U_1 y^*/l)$. A unidirectional magnetic field $\mathbf{b}^* = (b_x^*(y^*), 0)$ can be maintained, which satisfies Ohm's law (see (2.10) below), provided

$$-\frac{1}{l^2} \frac{d}{dy^*} (y^* b_x^*) = \frac{d^2 b_x^*}{dy^{*2}}. \quad (1.1a)$$

Here U_1 and l are chosen such that

$$\sigma \mu U_1 l = 1. \quad (1.1b)$$

Since the solution of (1.1*a*), which takes the form $b_x^* = -B_1(l/y^*)$, as $y^* \rightarrow \infty$, is

$$b_x^* = -B_1 e^{-y^{*2}/2l^2} \int_0^{y^*/l} e^{\frac{1}{2}\xi^2} d\xi, \quad (1.1c)$$

we may identify the length l with the thickness of the diffusion layer in which magnetic field

annihilation occurs. As before, the total ohmic dissipation per unit length of current sheet is of order

$$B_1^2/(\mu^2\sigma l) = U_1 B_1^2/\mu, \quad (1.2)$$

which is independent of the electrical conductivity and simply represents the Poynting flux towards the null plane. Moreover, since the flow is potential and since the Lorentz force

$$\mathbf{j}^* \times \mathbf{b}^* = -\nabla^* \left(\frac{1}{2\mu} b_x^{*2} \right) \quad (1.3)$$

can be balanced by part of the fluid pressure

$$\text{const} - \frac{1}{2}\rho u^{*2} - \frac{1}{2\mu} b_x^{*2} \quad (1.4)$$

the equation of motion (see (2.5) below) is also automatically satisfied.

The kinetic energy of a fluid flow is often increased by the rate of working $\mathbf{u}^* \cdot (\mathbf{j}^* \times \mathbf{b}^*)$ of the Lorentz force. In the above example, though the Lorentz force does work on the fluid, the character of the motion owes nothing to the presence of the magnetic field. Indeed, the fluid pressure adjusts its value so that the pressure force does work which is equal and opposite to the Lorentz force! In general, however, the Lorentz force cannot be balanced by pressure and truly magnetohydrodynamic (m.h.d.) motions ensue. In a highly conducting fluid an important new mechanism is introduced into the dynamics due to the presence of the magnetic field. It is the ability to propagate disturbances along magnetic field lines at the Alfvén velocity $\mathbf{b}^*/\sqrt{(\mu\rho)}$. Petschek (1964) has suggested that herein lies a mechanism whereby magnetic energy can be transformed rapidly into kinetic energy. Consider magnetic field convected, as above, slowly towards the plane of symmetry $y^* = 0$. Suppose, however, that the inflow velocity $-u_y^*$ varies with the coordinate x^* and takes its maximum value on a second plane of symmetry $x^* = 0$. In consequence a field line initially in the region $y^* > 0$ is convected up to the origin. There the line is severed and reconnected to a field line in the region $y^* < 0$, so forming an *X*-type magnetic field neutral point at the origin. The reconnected field lines are then convected away from the neutral point in the directions of both increasing and decreasing x^* . Evidently the origin is a singular point in the model and as such may be expected to be the source of disturbances. In fact, four lines emanate from the origin along which disturbances can propagate; the line in the quadrant ($x^* > 0, y^* > 0$) is OA in figure 1. At any point on the line OA disturbances propagate partially at the Alfvén velocity $-\mathbf{b}^*/\sqrt{(\mu\rho)}$ but are also convected with velocity \mathbf{u}^* . The net effect is propagation at the velocity $\mathbf{u}^* - \mathbf{b}^*/\sqrt{(\mu\rho)}$, tangent to OA. Across the line OA, often called an Alfvén line (see for example, Dix 1963), discontinuities of the tangential components of the magnetic field and flow velocity can be supported provided certain jump conditions are met (see (2.16*a*) below). As Petschek (1964) observed these discontinuities permit the magnetic energy density to drop dramatically across OA in favour of increased kinetic energy density. Moreover in a fluid of large but finite electrical conductivity considerable Ohmic dissipation occurs in thin layers, which we will call Alfvén boundary layers, of thickness $L\delta$ in the neighbourhood of OA. As the origin is approached, $L\delta$ decreases and two such layers, one on either side of the x^* axis, merge at a distance L from the origin to form the central diffusion region of width l (see figure 2). By contrast, it is the enhanced ohmic dissipation occurring in the central diffusion region alone (cf. (1.2) above) which was initially emphasized in the pioneering work of Dungey (1953, 1958) and Sweet (1958*a, b*); see also Parker (1963).

The discussion of Alfvén lines in the previous paragraph refers solely to incompressible fluids in which the sound speed is infinite. In a compressible fluid, the incompressible limit is only applicable when the gas pressure p_g is large compared with the magnetic pressure p_m . Astrophysical plasmas are, of course, highly compressible and in regions, where the magnetic fields are large, we may reasonably expect that $p_m \gg p_g$. Evidently the situation is now more complex, because, in addition to Alfvén wave propagation, disturbances can be propagated by magneto-acoustic waves. As the ratio p_m/p_g is increased from zero, Petschek & Thorne (1967)

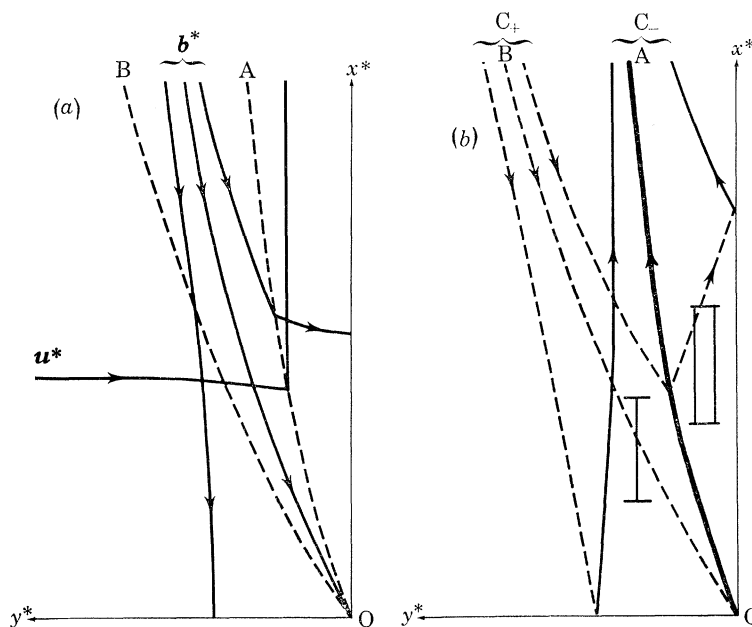


FIGURE 1. The streamlines u^* and the magnetic field lines b^* , which according to our solution describe the Petschek mechanism, are sketched in (a). The field line through the neutral point at the origin O is the separatrix. The corresponding streamlines for the characteristic velocities $v^*_\pm = u^* \pm b^*/\sqrt{\mu\rho}$ are sketched in (b) and the arrows indicate the direction in which information is propagated. The inflow region I is separated from the outflow region II by the Alfvén line OA . The structure of the mathematical problem changes also across the Alfvén line OB .

have suggested that, in general when the external magnetic field is non-uniform, as envisaged by Green & Sweet (1966), the Alfvén line discontinuity separates into a slow shock and an intermediate shock. Nevertheless, if the external magnetic field is almost uniform, as considered in this paper, the separation does not occur and we are left with the slow shock alone. In this case the analyses of the compressible and incompressible models are in many respects similar. The main difference results from the increase of gas pressure downstream of the shock, which leads to a corresponding density increase in the compressible case. The only quantitative differences in Petschek's original models were numerical factors dependent on the ratio of gas densities on either side of the shock. Though there are obvious shortcomings in restricting our investigation to incompressible fluids, it is reasonable to suppose that most of the important features of the reconnection process are represented well by the model.

It is widely believed that the rapid release of magnetic energy into kinetic energy and directly into heat by magnetic field line reconnection provides the energy source for solar flares. Whether the energy conversion occurs principally in the central diffusion region by the Sweet mechanism or across standing waves in the Alfvén boundary layers, as in the Petschek mechanism, depends

on the relative sizes of the length L of the central diffusion region and the overall length scale L_e characteristic of the flow. If L and L_e are comparable, then one has the Sweet mechanism. If, on the other hand, L is small compared with L_e , the ohmic heating in the Alfvén boundary layers alone is likely to exceed that in the central diffusion region by an order of magnitude.

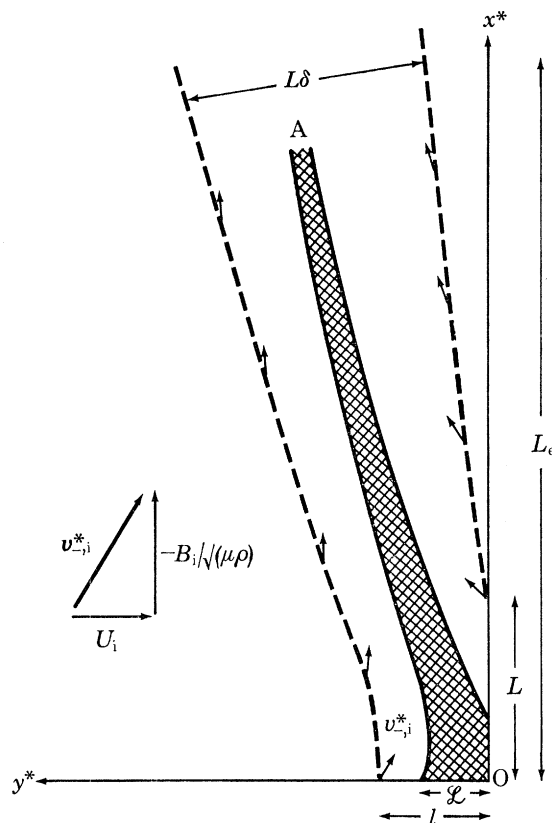


FIGURE 2. In the inflow region I, the Alfvén number M (see (3.38) and (3.3a)) increases as the origin O is approached and attains the value unity when $r^* = e^{\frac{1}{2}\pi} \mathcal{L}$. The solution in §§3–7 is only a valid approximation to the non-dissipative equations when M is large and so ceases to be valid when $r^* = O(\mathcal{L})$. Furthermore it is only valid outside a strip of width order \mathcal{L} which bounds the Alfvén line OA and is shaded in the figure (see §7). When dissipative effects are included the above approximate solution requires modification in certain small regions. In particular an Alfvén boundary layer forms about OA of thickness order $L\delta$, proportional to $\sqrt{r^*}$ (see (8.8)). It is confined by the convective effect of the characteristic velocity $\mathbf{v}_{*,i}^*$, which is indicated in the figure by the arrows on the dashed lines marking the edge of the layer. The central diffusion region of length order L and width order l is formed by the overlap of the Alfvén boundary layers in different quadrants. The ratio l/L is of order $M_1 (= U_i \sqrt{\mu\rho} / B_i)$, where the inflow values of the flow velocity U_i and magnetic field strength B_i are calculated at $x^* = 0$, $y^* = M_1 L (= O(l))$. Provided the ratio \mathcal{L}/l is small ($M_1 \ll 1$), the shaded region lies totally inside the Alfvén boundary layer, as indicated in the figure. When \mathcal{L}/l is large ($M_1 \gg 1$), however, the dashed lines only extend outside the shaded region at large distances from the origin. Finally, estimates of the reconnection rate M_e in §§3 and 10 are based on the overall size L_e of the region considered.

Yeh & Axford (1970), however, point out that though this concentrated electrical discharge may lead to remarkable effects, they should be regarded as secondary. The main effect is the lowering of the magnetic energy density across the Alfvén lines. In any event, the combined effect of ohmic dissipation and the rate of working of the Lorentz force in a steady state is measured by

$$-\nabla^* \cdot (\mathbf{E}^* \times \mathbf{b}^* / \mu), \quad (1.5)$$

where \mathbf{E}^* is the electric field (see, for example, Roberts (1967), p. 21). Since \mathbf{E}^* is constant (see §2 below), the conversion rate in a region bounded by a closed curve C is readily calculated from (1.5). It is

$$E^* \oint_C \mathbf{b}^* \cdot d\mathbf{x}^* / \mu = E^* I^*, \quad (1.6)$$

where I^* is the total electric current flowing across the region. Vasyliunas (1975) estimates this quantity for a variety of reconnection models in his recent review.

The main objection to the basic Sweet mechanism is that magnetic field line reconnection cannot release magnetic energy at a rate fast enough to produce solar flares (Parker 1963). Parker (1973*b*) points out, however, that dissipation rates may be increased considerably if small scale plasma instabilities are invoked. If that proves to be the case the objections to the Sweet mechanism evaporate. On the other hand, the estimate of the reconnection rate based on the Petschek mechanism is itself sufficiently large. Though the estimate depends on the electrical conductivity, its dependence is rather insensitive to the value of σ (see (10.7), (10.8) below). Ever since Petschek (1964) proposed his model with almost uniform external magnetic fields more detailed investigations have revealed several difficulties and certain curiosities. Of particular note is the reversed magnetic field phenomenon suggested by Green & Sweet (1966) for the more general case in which the external magnetic field is non-uniform and the second set of discontinuities advocated by Sonnerup (1970) and Yeh & Axford (1970). The net effect of these investigations and others is to render Petschek's original model suspect. The main aim of this paper is to allay these fears by placing Petschek's model on a sound mathematical basis. In achieving this goal the model developed here indicates the importance of various effects isolated by the recent investigations. These effects lead to minor discrepancies between our model and Petschek's. The differences are, however, by no means as dramatic as might have been suspected from the analyses of Green & Sweet (1966), Sonnerup (1970) and Yeh & Axford (1970).

In order to understand the Petschek mechanism in detail and to appreciate the main source of difficulty, it is useful to introduce the idea of characteristics. When all dissipations are neglected the m.h.d. equations are hyperbolic. Indeed, for the special case in which the total pressure (hydrodynamic plus magnetic) is constant, it is well known that

$$\mathbf{v}_\pm^* = \mathbf{u}^* \pm \mathbf{b}^* / \sqrt{(\mu\rho)} \quad (1.7)$$

is constant on C_\mp characteristics. These are the streamlines for the fictitious flow defined by the characteristic velocity \mathbf{v}_\mp^* . Sonnerup (1970) takes advantage of this simple property in the construction of his reconnection model (see §3 below). When the total pressure is non-uniform, the pressure gradient may be regarded as providing a continuous distribution of sources for the hyperbolic wave equation everywhere in the flow field. In other words, not only is information propagated along C_\pm characteristics at speeds \mathbf{v}_\pm^* but also at infinite speeds due to pressure responses. The latter mechanism is a manifestation of infinite sound speed in an incompressible fluid. Despite the added complication of the pressure term, the notion of characteristics is, however, important in our problem as they represent lines along which discontinuities can propagate. Indeed, we have already noted in describing Petschek's model that discontinuities persist on the characteristics emanating from the origin O .

A typical magnetic field and flow pattern is sketched in figure 1*a*, while the corresponding characteristics are sketched in figure 1*b*: the configuration is symmetric about the planes

$x^* = 0$, $y^* = 0$. Reconnection of magnetic field lines takes place at the origin O inside the small central diffusion region. The C_- characteristic OA (or second Alfvén line) divides the magnetic field and flow into two distinct regions. In the inflow region I the flow is sufficiently slow for inertia to be neglected and an approximate magnetostatic balance is achieved. In the narrow outflow region II the flow velocity is fast and comparable with the Alfvén velocity in region I. Moreover the C_+ characteristic OB (or first Alfvén line) separates region I into two parts, a fact which is not apparent from figure 1*a*. From figure 1*b*, it is clear that information is propagated from Oy^* to OB and from OB to Oy^* along C_- and C_+ characteristics respectively and similarly in region II between the lines OA and Ox^* . The situation is dramatically different in the remaining region. Here information is propagated along both C_+ and C_- characteristics from the line OB towards OA , but never in the opposite direction! Consequently, the upstream conditions to the left of OB can adjust (see also the discussion of the boundary conditions at infinity following (2.18) below) so that the flow and magnetic field vary continuously across the first Alfvén line, while the flow approaching the second Alfvén line is unaware of the impending discontinuity.

According to the steady non-dissipative equations the difference in character of the three regions distinguished above is not apparent, since \mathbf{v}_\pm^* can be replaced by $-\mathbf{v}_\pm^*$ without apparently altering the governing equations! For this reason both the models of Sonnerup (1970) and the exact similarity solutions of Yeh & Axford (1970) (see §3 below) permit discontinuities or singular behaviour to persist at both the Alfvén lines OA and OB . Indeed within the framework of their analyses both sets of discontinuities are necessary. If, however, we invoke time dependence or equivalently take account of the directional properties of the characteristics (see figure 1*b*), we see that discontinuities at the first Alfvén line are unrealistic. For, as Sonnerup (1970) has pointed out, the discontinuity across OB must be initiated externally and propagated towards the origin. In practice this requires four such discontinuities to have a common point of intersection (in our case the origin). Vasylunas (1975) has emphasized that this fortuitous coincidence is most unlikely but nevertheless suggests that Sonnerup's (1970) model may be the prototype for a class with faster reconnection rates than Petschek's (1964). For our unbounded models these discontinuities can only be initiated at infinity. Furthermore, even if the discontinuities did by chance intersect, Yeh & Axford's model still fails; as shown in §8 and already noted by Vasylunas (1975). Once the effects of finite electrical conductivity and/or viscosity are taken into account the solutions on either side of OB cannot be connected. The exception is Sonnerup's (1970) solution, which fails in an unbounded region, but remains valid if the discontinuity is initiated at a finite distance from the origin.

In §2 the governing equations and boundary conditions appropriate to an unbounded region are established in dimensionless form. The mathematical problem is characterized by three dimensionless numbers, namely the Alfvén number M_1 , the magnetic Reynolds number $R_{m,1}$ and the Reynolds number $R_{f,1}$ (see (2.3), (2.12) and (2.8) respectively), the subscript i referring to values just outside the diffusion region on the y -axis. In §§3–7 we are concerned with the non-dissipative equations, for which the Alfvén number M_1 is the only relevant parameter (see (2.15) below) and is assumed to be of order 1 or smaller. A solution (3.2) is sought, almost self-similar in form, such that a magnetostatic balance is achieved in the inflow region and there is no singular behaviour at OB . Analytic progress is made by finding asymptotic solutions of the resulting equations, valid when the parameter $R = \ln(r^*/\mathcal{L})$, where the ratio \mathcal{L}/L only depends on M_1 (see (3.36) below) and r^* is the distance from its origin, is much greater than

unity. There is in essence only one independent solution and for this M_1 provides a measure of the anticipated size of the diffusion regions.

The prime consideration in the development of the reconnection model in § 3 is that no discontinuity or singular behaviour should be permitted at the first Alfvén line OB. This condition is built neither into Petschek's original analysis nor into the more recent refinements of Vasyliunas (1975) and Roberts & Priest (1975). To the order of accuracy considered in their analyses, the flow is irrotational and the magnetic field is current free in the inflow region I. Consequently the condition at OB is automatically satisfied and its importance is not apparent. We find, however, that the condition severely restricts the solution to the reconnection problem and would expect that the development of the above analyses to higher orders would encounter serious difficulties. A wide class of similarity solutions is attempted in appendix A but none are found to satisfy the required condition at OB. The analysis suggests, however, that the solution in the inflow region I is almost described by the similarity formulation advocated by Yeh & Axford (1970) (see (3.2) below). In fact, their similarity form describes the Petschek mechanism locally and it is only over very large radial distances that there is any noticeable variation of the similarity functions through their dependence on the parameter R . To lowest order a state of constant total pressure is realized as in Sonnerup's (1970) model and the magnetic field lines and streamlines are almost straight. Slight bending of the field lines, which is evident at a higher order, permits Petschek's configuration to be realized without additional discontinuities across the Alfvén line OB. In the zero order approximation at least, the Alfvén lines collapse on to the axis of symmetry and so the model, regarded as a member of the Yeh & Axford (1970) class of similarity solutions is a degenerate case. When the finite width of the outflow region II between the Alfvén line OA and the x^* -axis is taken into account, the details of the solution can be deduced most easily by the introduction of a boundary layer coordinate (see (3.14*a*) below). The results confirm all the assumptions and principal force balances predicted by Petschek (1964). It is found, however, that the Alfvén line OA is not straight but curves slowly away from the incoming flow. Consequently the Alfvén number M (see (3.38*c*) below), which provides the important measure of the merging (or reconnection) rate of the magnetic field lines, decreases with distance from the origin. Since variations with distance are small, the Alfvén number is effectively constant and the Alfvén line is effectively straight on any prescribed length scale and, in particular, on the largest length L_e of interest. On this large length scale Petschek's estimate of the maximum reconnection rate is confirmed to within a factor 2 (see (10.9) and figure 8 below).

To a high order of accuracy the magnetic field and fluid velocity in the inflow region I are free of electric current and vorticity. That part of the solution which is potential can be approximated uniformly throughout region I by complex potentials. These are developed in § 4. Since the magnetic field here is not completely uniform, a small positive radial total pressure gradient is predicted (see (4.19*e*) below). The pressure gradient persists into the outflow region II and its influence on the flow there is investigated in § 5. In particular, it is found to induce singular behaviour in the flow and magnetic field near the Alfvén line OA as predicted by Yeh & Axford (1970). We find, however, that the singularity is not as severe as their model might suggest (see §§ 7 and 8 below).

The analysis in §§ 3–7 yields two technical difficulties. First, the expansion procedures reveal the existence of an arbitrary constant α (see (5.11) below), which may be absorbed into the definition of M_1 . The existence of the constant, which reflects a similarity property of the solu-

tions, leads to a degeneracy which is overcome only by the introduction of the $\ln R$ terms in §§ 4 and 5 (see, for example, (4.19), (5.1) below). Second, the asymptotic expansions break down in a thin region containing the Alfvén line OA, which we call an Alfvén layer. Here the singular behaviour of the flow and magnetic field is associated with singular concentrations of vorticity and electric current. The lack of significant vorticity and electric current in region I implies, therefore, that terms of a high order must be considered before any singular behaviour to the left of the Alfvén line OA can be predicted. These small concentrations of vorticity and electric current (see (6.39) and (6.32) respectively) are determined by the lengthy analysis of § 6. With the exception of the Alfvén layer discussed in § 7, the results of § 6 conclude the development of solution to the non-dissipative equations and at the same time indicate how the analysis may be systematically extended to any required order.

As remarked earlier, dissipative effects are important in Alfvén boundary layers[†] located near the centre of the Alfvén layers. In § 8 the structures of these Alfvén boundary layers is determined and for the particular case $M_1 \ll 1$ the highly complex central diffusion region, where the Alfvén boundary layers merge, is described qualitatively. In § 9 the applicability of our solution to the case $M_1 = O(1)$ is discussed, while in § 10, the principal conclusions are summarized and bounds on the reconnection rate are derived.

2. THE MATHEMATICAL PROBLEM

A steady, incompressible, two dimensional hydromagnetic flow of a fluid, density ρ , is referred to cylindrical coordinates (r^*, θ, z^*) . The line $\theta = 0$ is the positive x^* axis. The magnetic field $\mathbf{b}^* = (b_r^*, b_\theta^*)$ and fluid velocity $\mathbf{u}^* = (u_r^*, u_\theta^*)$ lie entirely in the r^*, θ plane and depend only on the coordinates r^* and θ . On the other hand the electric field \mathbf{E}^* is assumed to lie in the z^* direction and, because of the Maxwell equation $\text{curl } \mathbf{E}^* = 0$, E_z^* is constant independent of both position and time.

It is convenient to adopt the length L of the central diffusion region as our basic length scale and to introduce the non-dimensional position vector

$$\mathbf{x} = \mathbf{x}^*/L. \quad (2.1)$$

The magnetic field and flow velocity are made dimensionless by the change of variables

$$\mathbf{b}^*/B_1 = M_1^{\frac{1}{2}} \mathbf{b}, \quad \mathbf{u}^*/U_1 = M_1^{-\frac{1}{2}} \mathbf{u}, \quad (2.2)$$

where B_1 is the magnetic field strength at the edge of the diffusion region and U_1 is the inflow velocity. The constant M_1 is chosen so that $|\mathbf{u}|$ equals $|\mathbf{b}|$, when the fluid velocity equals the Alfvén speed. It is the Alfvén number

$$M_1 = U_1/V_1, \quad (2.3a)$$

where

$$V_1 = B_1/\sqrt{(\mu\rho)} \quad (2.3b)$$

is the Alfvén velocity based on the magnetic field strength B_1 . In terms of the magnetic vector potential χ and stream function ψ the magnetic field and fluid velocity may be written as

$$\mathbf{b} = \left(\frac{1}{r} \frac{\partial \chi}{\partial \theta}, -\frac{\partial \chi}{\partial r} \right), \quad \mathbf{u} = \left(\frac{1}{r} \frac{\partial \psi}{\partial \theta}, -\frac{\partial \psi}{\partial r} \right). \quad (2.4)$$

[†] The terminology here differs slightly from that adopted by Hughes & Young (1966), who abbreviate the name Alfvén boundary layer to Alfvén layer. We use the latter term to include the more extensive singular region bounding the Alfvén line.

Substitution of (2.1)–(2.4) into the equation of motion yields (see, for example, Yeh & Axford 1970)

$$-\frac{\partial(\psi, u_r)}{\partial(r, \theta)} - u_\theta^2 = -r \frac{\partial p}{\partial r} - \frac{\partial(\chi, b_r)}{\partial(r, \theta)} - b_\theta^2 - (M_1^{\frac{1}{2}} R_{t,1})^{-1} \frac{\partial \omega}{\partial \theta}, \quad (2.5a)$$

$$-\frac{\partial(\psi, u_\theta)}{\partial(r, \theta)} + u_r u_\theta = -\frac{\partial p}{\partial \theta} - \frac{\partial(\chi, b_\theta)}{\partial(r, \theta)} + b_r b_\theta + (M_1^{\frac{1}{2}} R_{t,1})^{-1} r \frac{\partial \omega}{\partial r}, \quad (2.5b)$$

where $\rho U_1 V_1 \{p - \frac{1}{2} b^2\}$ is the hydrodynamic pressure, p is the non-dimensional total pressure,

$$\frac{\partial(\psi, \chi)}{\partial(r, \theta)} = \frac{\partial \psi}{\partial r} \frac{\partial \chi}{\partial \theta} - \frac{\partial \psi}{\partial \theta} \frac{\partial \chi}{\partial r} \quad (2.6)$$

is the Jacobian, $(L/U_1) \omega^* = M_1^{-\frac{1}{2}} \omega = -M_1^{-\frac{1}{2}} \nabla^2 \psi$ (2.7)

is the dimensionless vorticity and $R_{t,1} = LV_1/\nu$ (2.8)

is the Reynolds number (ν is the kinematic viscosity). Here it is anticipated that fluid escapes from the central diffusion region at the Alfvén velocity V_1 . According to the frozen field equation, the constant electric field can be determined by the conditions at the edge of the diffusion region. It is

$$E_z^* = U_1 B_1. \quad (2.9)$$

Elsewhere Ohm's law becomes

$$(M_1^{\frac{1}{2}} R_{m,1})^{-1} j = 1 + (\mathbf{u} \times \mathbf{b})_z, \quad (2.10a)$$

or equivalently $-\frac{1}{r} \frac{\partial(\psi, \chi)}{\partial(r, \theta)} = 1 + (M_1^{\frac{1}{2}} R_{m,1})^{-1} \nabla^2 \chi$ (2.10b)

where $(\mu L/B_1) j^* = M_1^{\frac{1}{2}} j = -M_1^{\frac{1}{2}} \nabla^2 \chi$ (2.11)

is the dimensionless electric current and

$$R_{m,1} = LV_1 \mu \sigma \quad (2.12)$$

is the magnetic Reynolds number. The width

$$l = (M_1 R_{m,1})^{-1} L \quad (2.13)$$

of the central diffusion region is determined by the condition that the Reynolds number $lU_1 \mu \sigma$ based on the inflow velocity is unity (see (1.1b)).

Since the total pressure $p = p_g + p_m$ is continuous everywhere, the value of the gas pressure in the central diffusion region, which is at least comparable with the magnetic pressure, must be of order $B_1^2/2\mu$. Consequently the outflow, driven by the downstream pressure gradient, has speed comparable with Alfvén velocity V_1 . Furthermore, since the volume flux per unit width into and out of the central diffusion region are of order $U_1 l$ and $V_1 l$ respectively, mass conservation indicates that

$$l/L = O(U_1/V_1) = O(M_1). \quad (2.14a)$$

Together with (2.13), the result yields the further estimate

$$R_{m,1} = O(M_1^{-2}). \quad (2.14b)$$

The rate of merging of magnetic field is either slow ($M_1 \ll 1$) or fast ($M_1 = O(1)$). In the former case the analysis of this paper is valid everywhere outside the central diffusion region. In the latter case L and \mathcal{L} (see (3.36) below) are both of order l and our solution is only valid when

In (r^*/l) is large. Since l is extremely small it may reasonably be supposed that our solution will be valid throughout most of the reconnection region except for a relatively small neighbourhood of the origin. In either case we find that the importance of dissipative processes at a distance r^* is measured by $R_m = (r^*L)(M_1/M)^{1/2}R_{m,1}$ (see (8.8*b*)), where M is the local Alfvén number. Since the local magnetic Reynolds number R_m increases indefinitely, as $r^* \rightarrow \infty$, dissipation is negligible almost everywhere in the flow. The ensuing approximations to the equations are effected by neglecting viscosity and Ohmic diffusion and setting

$$1/R_{t,1} = 1/R_{m,1} = 0. \quad (2.15)$$

Dissipation, however, is important in an Alfvén boundary layer containing the second Alfvén line, at which

$$\psi = \chi, \quad (2.16a)$$

indicated by the line OA in figure 1. Across this diffusion region, which has zero width in the limit (2.15), discontinuities in the tangential components of \mathbf{u} and \mathbf{b} are permitted. The normal components are, however, continuous together with the total pressure p . Within the framework of our steady state model our analysis also shows that an Alfvén boundary layer cannot be supported across the first Alfvén line, at which

$$\psi = -\chi, \quad (2.16b)$$

indicated by the line OB in figure 1. Here no discontinuities are permitted.

Owing to the symmetry the flow and magnetic field are investigated only in the quadrant $0 \leq \theta \leq \frac{1}{2}\pi$. Magnetic flux χ is measured from the separatrix, which is the magnetic field line passing through the neutral point at the origin O and on which χ is zero. To the right of this line the magnetic field is reconnected and χ is positive, while to the left χ is negative. Symmetry conditions require that the magnetic field is normal to the lines $\theta = 0$ and $\frac{1}{2}\pi$. Consequently χ takes its maximum and minimum values at $\theta = 0$ and $\frac{1}{2}\pi$ respectively where

$$\partial\chi/\partial\theta = 0 \quad (\theta = 0, \frac{1}{2}\pi). \quad (2.17a)$$

Moreover, the lines $\theta = 0$ and $\frac{1}{2}\pi$ are streamlines and are therefore lines of constant ψ . Since the streamlines intersect at the origin the value of ψ on each is the same and can be chosen arbitrarily. We choose

$$\psi = 0 \quad (\theta = 0, \frac{1}{2}\pi), \quad (2.17b)$$

so that elsewhere in the quadrant ψ is positive. Inspection of figure 3 indicates that the Alfvén line OA is located in the region of reconnected magnetic field. Since the character of the magnetic field and flow changes dramatically across this line we call the regions to the left and right of it,

$$\begin{aligned} \text{region I: } & \frac{1}{2}\pi \geq \theta > \Theta \quad (\psi > \chi), \\ \text{region II: } & \Theta > \theta \geq 0 \quad (\chi > \psi), \end{aligned} \quad (2.18)$$

respectively. Here Θ is not a constant but a function of radial distance from the origin.

In an inviscid, perfectly conducting fluid, it is impossible to prescribe precise boundary conditions on the flow and magnetic field, as $r^* \rightarrow \infty$. This difficulty is peculiar to the problem of finding steady state solutions and is avoided if a time-dependent problem is considered. In that case disturbances can only propagate as Alfvén waves up to a finite distance of order $V_1 t^*$ in time t^* . As t^* tends to ∞ and a steady state is approached, the particular conditions initially applied at infinity may be ultimately disrupted. Consequently, in a steady state the prescription of boundary

conditions at infinity may overpose the problem. One assumption is made, however, namely that inertia is insignificant in the inflow region, as $r^* \rightarrow \infty$.

In the following sections no attempt is made to determine a complete solution to the problem posed everywhere in the fluid. In particular, the detailed character of the central diffusion region is not determined. It is believed, however, that the rôle of this region is passive inasmuch as it adjusts to the inflow conditions. The external conditions at some large reference distance L_e , however, are also influenced by the inflow conditions immediately outside the central diffusion region. Consequently the inflow speed at the distance L_e cannot necessarily be any fraction M_e of the local Alfvén speed (see also Priest & Cowley 1975). In the case of slow merging rates ($M_i \ll 1$), it would appear natural, following Petschek (1964) and Vasyliunas (1975), to seek asymptotic expansions of the solution outside the central diffusion region which are based on M_i small. In order to obtain asymptotic expansions which are uniformly valid as $r^* \rightarrow \infty$, it transpires instead to be more convenient to attempt similarity solutions, whose accuracy improves in this limit.

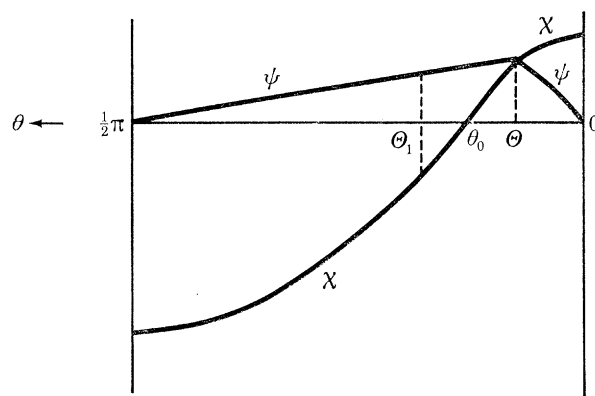


FIGURE 3. The stream function ψ and the magnetic potential χ are plotted against θ , for fixed r , in the interval $0 \leq \theta \leq \frac{1}{2}\pi$ in accordance with the solution sketched in figure 1. The Alfvén lines OA and OB are located at $\theta = \Theta$ and Θ_1 respectively. The separatrix at which $\chi = 0$, is located at $\theta = \theta_0$. Only the boundary conditions illustrated by the graphs and not the shape of the curves are assumed in the derivation of our solution.

Only four assumptions are made in this paper, namely

- (i) The inflow Alfvén number M_i is of order 1 or smaller.
- (ii) On the length scale L_e , the inflow magnetic Reynolds number $R_{m,e}$ is large.
- (iii) The solution has similarity form on any length scale lying between L and L_e (the 'local' similarity assumption).
- (iv) The magnetostatic approximation holds in the inflow region, as $r^* \rightarrow \infty$.

Assumptions (i) and (ii), together with the estimates (2.14*b*), (10.7), (10.8) imply that the ratio L_e/L is large consistent with the similarity assumption (iii) and that the inflow Alfvén number based on the external conditions is small even when M_i is of order 1. Furthermore, we conclude on the basis of assumption (iii) and (iv) that the magnetic field in the inflow region is force-free and almost uniform at large distances. All similarity models in which the gas pressure is comparable with the magnetic pressure (i.e. the wider class of magnetostatic models envisaged in (iv)) in the inflow region are rejected (see appendix A). Finally since the external conditions for steady state models cannot be prescribed arbitrarily, we may speculate that the non-uniform external conditions envisaged by Green & Sweet (1966) cannot be maintained and that the difficulties that they encounter will not arise.

3. THE SIMILARITY SOLUTION

When the total pressure is constant everywhere in the fluid, solutions of the steady non-dissipative equations governing the flow are extremely simple and have the property that the characteristic velocities $\mathbf{u} \pm \mathbf{b}$ are constant on C_{\mp} characteristics. The result implies that the C_{\pm} characteristics are straight and \mathbf{u} , \mathbf{b} are constant everywhere except possibly for discontinuities across isolated C_{\pm} characteristics. Sonnerup (1970) has invoked this property to advantage in his solution of the reconnection problem. Thus in the quadrant illustrated in figure 1, Sonnerup allows for discontinuities at one C_+ and one C_- characteristic, while elsewhere the flow and magnetic field are uniform. When both characteristics pass through the neutral point the solution is of self-similar form and a special case of the complete class of exact similarity solutions derived by Yeh & Axford (1970), in which total pressure is not necessarily constant. All these solutions unfortunately fail to satisfy the condition that there should be discontinuities across only the Alfvén line OA (see figure 1).

The most important feature of Yeh & Axford's (1970) similarity solution ($n = 0$ in (3.1) below) is that no natural length \mathcal{L} , at which inertia and Lorentz forces are comparable, is defined (this is not the case when $n \neq 0$). In fact, the magnetic field and flow velocity are constant on lines of constant θ . Consequently along these lines the relative importance of the inertia to the Lorentz forces is everywhere the same. Yeh & Axford's model also has the undesirable feature for many applications that the ratio of the gas to magnetic pressure increases indefinitely with distance. By contrast, in common with Petschek (1964), we search for solutions in which inertial forces in the inflow region are negligible by comparison with the Lorentz force so that here an approximate magnetostatic balance is achieved. (It turns out that to a high order of approximation the magnetic field is force free; $\mathbf{j} \times \mathbf{b} = 0$.) Upon neglect of the inertia term from the equation of motion (2.5), the reduced non-dissipative equations admit a wide class of similarity solutions which take the form†

$$\psi = r^{1-n}g(\theta), \quad \chi = r^{1+nf}(\theta), \quad p = r^{2n}P(\theta) \quad (n > 0). \quad (3.1)$$

Provided n is positive and r large, the representation (3.1) is compatible with the neglect of inertia. Now according to (2.2) and (2.4), g and f are typically of order $M_1^{\frac{1}{2}}$ and $M_1^{-\frac{1}{2}}$ respectively. It follows that the magnetostatic approximation ceases to be valid at the distance \mathcal{L} of order $M_1^{1/2n}L$, where ψ and χ are typically the same size. Since l is of order M_1L , the similarity solution is likely to be valid right up to the central diffusion region provided $\mathcal{L} \ll l$ or equivalently $M_1 \ll 1$. Even for M_1 of order 1, however, the region near the origin not described by the similarity solution is likely to be small comparable in size to the diffusion region.

The possible implications of a solution taking the form (3.1) are discussed at length in appendix A where in order not to obscure the main issues it is assumed that M_1 is order 1. The case (ii), described there, is closest to the accepted picture of the reconnection process. For that case, (3.1) provides a first approximation to the solution everywhere except in the vicinity of the outflowing jet near $\theta = 0$. Here the Alfvén line OA is located at $\theta = \Theta$ where Θ is order $r^{-2n/(1+2n)}$ and tends to zero, as $r \rightarrow \infty$. When θ/Θ is of order 1, inertia and Lorentz forces are comparable. The resulting boundary layer structure may then be described by a new similarity solution for which a convenient similarity variable is $r^{2n/(1+2n)}\theta$.

† The more general class based on $\psi = r^p g(r^q \theta)$, where p and q (> 0) are constants, is applicable only in thin boundary layer regions (see the following paragraph and Appendix A).

As in Yeh & Axford's (1970) class of exact similarity solutions, no solution is found in either case (ii) or (iii) which does not suffer discontinuity or exhibit some singular behaviour at the first Alfvén line OB. The solutions (3.1) are thus rejected. The main source of difficulty appears to evaporate in case (ii), as $n \rightarrow 0$, and suggests that the $n = 0$ similarity form is close in some sense to the actual solution. We are led to speculate, therefore, that ψ , χ and p are given by

$$\psi = rg(R, \theta), \quad \chi = rf(R, \theta), \quad p = p(R, \theta), \quad (3.2)$$

where g , f and p vary weakly with respect to radial distance through their dependence on

$$R = R_0 + \ln r = \ln(r^*/\mathcal{L}). \quad (3.3a)$$

$$\text{The arbitrary constant} \quad R_0 = \ln(L/\mathcal{L}) \quad (3.3b)$$

is to be chosen later (see (3.36) below) at our convenience. Guided by the results of appendix A, case (ii), we anticipate that the solution is valid everywhere, except near $\theta = 0$, for sufficiently large R and assume that

$$\Theta(R) \rightarrow 0, \quad \text{as } R \rightarrow \infty. \quad (3.4)$$

(a) *The equations*

In terms of the new variables the velocity and magnetic field are

$$\mathbf{u} = \left[\frac{\partial g}{\partial \theta}, -\left(g + \frac{\partial g}{\partial R}\right) \right], \quad \mathbf{b} = \left[\frac{\partial f}{\partial \theta}, -\left(f + \frac{\partial f}{\partial R}\right) \right]. \quad (3.5)$$

The vorticity and electric current are

$$\omega = -(1/r) \mathcal{D}g, \quad j = -(1/r) \mathcal{D}f, \quad (3.6a)$$

$$\text{where} \quad \mathcal{D} = \partial^2/\partial\theta^2 + (1 + \partial/\partial R)^2. \quad (3.6b)$$

In the case of negligible viscosity ($\nu = 0$) the equation of motion (2.5) becomes

$$-g\mathcal{D}g + \left[g \frac{\partial^2 g}{\partial R^2} - \left(\frac{\partial g}{\partial R}\right)^2 \right] - \frac{\partial(g, \partial g/\partial \theta)}{\partial(R, \theta)} = -\frac{\partial p}{\partial R} - f\mathcal{D}f + \left[f \frac{\partial^2 f}{\partial R^2} - \left(\frac{\partial f}{\partial R}\right)^2 \right] - \frac{\partial(f, \partial f/\partial \theta)}{\partial(R, \theta)}, \quad (3.7a)$$

$$\left[g \frac{\partial^2 g}{\partial R \partial \theta} - \frac{\partial g}{\partial R} \frac{\partial g}{\partial \theta} \right] + \frac{\partial(g, \partial g/\partial R)}{\partial(R, \theta)} = -\frac{\partial p}{\partial \theta} + \left[f \frac{\partial^2 f}{\partial R \partial \theta} - \frac{\partial f}{\partial R} \frac{\partial f}{\partial \theta} \right] + \frac{\partial(f, \partial f/\partial R)}{\partial(R, \theta)}. \quad (3.7b)$$

Restricting attention to the case of infinite conductivity, Ohm's law (2.10) reduces to the frozen field equation

$$-g \frac{\partial f}{\partial \theta} + f \frac{\partial g}{\partial \theta} - \frac{\partial(g, f)}{\partial(R, \theta)} = 1. \quad (3.8)$$

(b) *Lowest order outer solution*

Far from the origin we anticipate that $(1/g) \partial g/\partial R$, $(1/f) \partial f/\partial R$ and $(1/p) \partial p/\partial R$ are all small and order R^{-1} . In a first approximation to equations (3.5) to (3.8), therefore, it is reasonable to neglect all partial derivations with respect to R except for the term $-\partial p/\partial R$ in (3.7a), which determines the radial pressure gradient. The reduced equations are then identical with the equations investigated by Yeh & Axford (1970). Since by hypothesis inertia and therefore the left hand side of (3.7) is assumed unimportant at large R , (3.7a) becomes

$$0 = -\frac{\partial p}{\partial R} - f \left(\frac{\partial^2 f}{\partial \theta^2} + f \right). \quad (3.9)$$

Consequently p is of order Rf^2 and hence (3.7b) is dominated by the term $-\partial p/\partial\theta$. It follows that to lowest order p is independent of θ and so (3.9) can be integrated once yielding

$$(\partial f/\partial\theta)^2 = f_{\max}^2 - 2(\partial p/\partial R) \ln(f/f_{\max}) - f^2, \quad (3.10)$$

where $-f_{\max}$ is the maximum value of $-f$ achieved at $\theta = \frac{1}{2}\pi$ (see (2.17a)). As in appendix A, case (i), if $\partial p/\partial R$ is negative f is never zero and so there is no reconnection. Provided $\partial p/\partial R$ is positive, however, reconnection is possible and the reconnected magnetic field is bounded by the curve $\theta = \theta_0$, where

$$\theta_0 = \frac{1}{2}\pi - \int_0^1 d\tau/\sqrt{(1 - 2((\partial p/\partial R)/f_{\max}^2) \ln \tau - \tau^2)}, \quad (3.11)$$

and $f(\theta_0) = 0$. Now, the magnetostatic approximation is effected by the limit $g/f \rightarrow 0$, as $R \rightarrow \infty$. This limit is achieved everywhere except at the angle $\theta = 0$, to which we assume both θ_0 and Θ converge, as $R \rightarrow \infty$ (see (3.4) and figure 2). Since the integral in (3.11) is less than $\frac{1}{2}\pi$, the limits

$$\theta_0 \rightarrow 0 \quad \text{and} \quad (\partial p/\partial R)/f_{\max}^2 \rightarrow 0 \quad (3.12)$$

are equivalent. Consequently in the lowest order approximation to (3.7a) the radial pressure gradient is negligible. Upon neglect of $\partial p/\partial R$ in (3.9) it becomes clear that the solution which satisfies the boundary condition, $\partial f/\partial\theta = 0$ at $\theta = 0$, (see (2.17a)) is

$$f = -a \sin \theta, \quad (3.13a)$$

where a is as yet an undetermined function of R . The corresponding lowest order approximation to the frozen field equation (3.8), which satisfies the boundary condition, $g(\frac{1}{2}\pi) = 0$ (see (2.17b)), is

$$g = (1/a) \cos \theta. \quad (3.13b)$$

(c) Inner region equations

Though the boundary conditions at $\theta = \frac{1}{2}\pi$ have been satisfied, no attempt has been made to satisfy the boundary conditions (2.17) at $\theta = 0$. In the vicinity of $\theta = 0$ the neglect of inertia is unjustified and consequently the approximations leading to (3.13) breakdown. In order to develop an approximate solution in the neighbourhood of $\theta = 0$, it is convenient to stretch the angle θ by introduction of the boundary layer coordinate

$$\xi = \theta/\Theta \quad (3.14a)$$

and to make the change of variables

$$f = F(R, \xi), \quad g = G(R, \xi), \quad p = P(R, \xi). \quad (3.14b)$$

The choice of boundary layer coordinate ensures that the Alfvén line OA at which discontinuities are permitted is located at $\xi = 1$. The transformation from the outer R, θ coordinates to the inner R, ξ coordinates is facilitated by the identities

$$\begin{bmatrix} \frac{\partial R}{\partial R} & \frac{\partial \xi}{\partial R} \\ \frac{\partial R}{\partial \theta} & \frac{\partial \xi}{\partial \theta} \end{bmatrix} = \begin{bmatrix} 1 & -\frac{\Theta'}{\Theta} \xi \\ 0 & \frac{1}{\Theta} \end{bmatrix} \quad \text{and} \quad \frac{\partial(f, g)}{\partial(R, \theta)} = \frac{1}{\Theta} \frac{\partial(F, G)}{\partial(R, \xi)}, \quad (3.15)$$

where the prime denotes differentiation ($\Theta' = d\Theta/dR$).

In terms of the boundary layer coordinates the velocity and magnetic field are

$$\begin{aligned} \mathbf{u} &= \left[\frac{1}{\Theta} \frac{\partial G}{\partial \xi}, - \left(G + \frac{\partial G}{\partial R} - \frac{\Theta'}{\Theta} \xi \frac{\partial G}{\partial \xi} \right) \right], \\ \mathbf{b} &= \left[\frac{1}{\Theta} \frac{\partial F}{\partial \xi}, - \left(F + \frac{\partial F}{\partial R} - \frac{\Theta'}{\Theta} \xi \frac{\partial F}{\partial \xi} \right) \right]. \end{aligned} \quad (3.16)$$

The radial component (3.7a) of the equation of motion becomes

$$\begin{aligned} G \frac{\partial^2 G}{\partial \xi^2} + \Theta \frac{\partial(G, 1/\Theta \partial G/\partial \xi)}{\partial(R, \xi)} + \Theta^2 \left(G + \frac{\partial G}{\partial R} - \frac{\Theta'}{\Theta} \xi \frac{\partial G}{\partial \xi} \right)^2 \\ = \Theta^2 \left(\frac{\partial P}{\partial R} - \frac{\Theta'}{\Theta} \xi \frac{\partial P}{\partial \xi} \right) + F \frac{\partial^2 F}{\partial \xi^2} + \Theta \frac{\partial(F, 1/\Theta \partial F/\partial \xi)}{\partial(R, \xi)} + \Theta^2 \left(F + \frac{\partial F}{\partial R} - \frac{\Theta'}{\Theta} \xi \frac{\partial F}{\partial \xi} \right)^2. \end{aligned} \quad (3.17a)$$

From the θ -component (3.7b) of the equation of motion it is sufficient to notice that

$$\frac{\partial P}{\partial \xi} = O\left(\max\left[\frac{G^2}{R}, \frac{F^2}{R}\right]\right). \quad (3.17b)$$

Consequently for small Θ (large R), the boundary layer approximation, in which P is assumed independent of ξ , will be well founded. Finally the frozen field equation (3.8) transforms almost trivially giving

$$-G \frac{\partial F}{\partial \xi} + F \frac{\partial G}{\partial \xi} - \frac{\partial(G, F)}{\partial(R, \xi)} = \Theta. \quad (3.18)$$

(d) *Lowest order inner solution*

As in the case of the outer solution described above equations (3.16)–(3.18) are approximated on the basis that $\partial/\partial R$ is order R^{-1} . Thus retention of the dominant terms in (3.17a) yields the equation

$$G \frac{\partial^2 G}{\partial \xi^2} = F \frac{\partial^2 F}{\partial \xi^2} + \Theta^2 P' \quad (P = P(R)), \quad (3.19)$$

which describes the balance of inward convection of radial momentum (u_θ/r) ($\partial u_r/\partial \theta$), the corresponding magnetic term (b_θ/r) ($\partial b_r/\partial \theta$) and the radial total pressure gradient $\partial p/\partial r$. Similarly (3.18) reduces to

$$-G \frac{\partial F}{\partial \xi} + F \frac{\partial G}{\partial \xi} = \Theta. \quad (3.20)$$

Differentiating (3.20) with respect to ξ and eliminating $\partial^2 G/\partial \xi^2$ from the result and (3.19) yields

$$(G^2 - F^2) \frac{\partial^2 F}{\partial \xi^2} = \Theta^2 P' F. \quad (3.21)$$

The equation has two singular points $\xi = 1, \xi_B$ at which $F(1) = G(1)$ and $F(\xi_B) = -G(\xi_B)$. The former corresponds to the Alfvén line OA; the latter corresponds to the Alfvén line OB. Since our solution to (3.19) and (3.20) must be analytic at the singular point $\xi = \xi_B$, it follows that $\Theta^2 P' F(\xi_B)$ is zero. Both Θ and $F(\xi_B)$ are non-zero, however, and so we must conclude that the pressure gradient is negligible in the first approximation. It follows that $\partial^2 F/\partial \xi^2 = 0$ everywhere except at the point $\xi = 1$. At this point F and G are continuous, while $\partial F/\partial \xi$ and $\partial G/\partial \xi$ may suffer discontinuities. The former condition ensures the continuity to lowest order of the normal component of magnetic field and velocity across the Alfvén line, while the latter condition allows for the possibility that the tangential components of these quantities may jump in value.

In region II, (3.19) and (3.20) constitute a third order pair of differential equations having three boundary conditions, namely $G = \partial F/\partial \xi = 0$ at $\xi = 0$ and $F = G$ at $\xi = 1$. The unique solution is

$$G = \sqrt{\theta} \xi, \quad F = \sqrt{\theta} \quad \text{in II.} \quad (3.22a)$$

The solution exterior to the Alfvén line has the two boundary conditions $F = G = \sqrt{\theta}$ at $\xi = 1$. The solution is restricted further by the requirement that, as $\xi \rightarrow \infty$, G matches with g , as $\theta \rightarrow 0$. The latter constraint implies that G tends to a function of R alone, as $\xi \rightarrow \infty$. Hence the required solution is unique and given by

$$G = \sqrt{\theta}, \quad F = \sqrt{\theta} (2 - \xi) \quad \text{in I,} \quad (3.22b)$$

from which it can be seen that the Alfvén line OB, at which $F = -G$, is situated approximately at $\xi = 3$. Now, as $\xi \rightarrow \infty$, G and F have the asymptotic forms

$$G \rightarrow \sqrt{\theta}, \quad F \rightarrow -\sqrt{\theta} \xi = -\theta/\sqrt{\theta}, \quad (3.23a)$$

while, as $\theta \rightarrow 0$, g and f have the asymptotic forms

$$g \rightarrow 1/a, \quad f \rightarrow -a\theta. \quad (3.23b)$$

Evidently matching is achieved if

$$a = 1/\sqrt{\theta}. \quad (3.24)$$

Unfortunately, since θ is still an unknown function of R , the lowest order solution is still not fixed.

(e) *Higher order inner and outer solutions in region I*

Continuity of magnetic field and fluid velocity across the Alfvén line OB ($\xi = 3$)[†] is the vital condition which ultimately determines the solution uniquely. We, therefore, proceed to determine a better approximation to G and F in region I by setting

$$G = \sqrt{\theta} + \tilde{G}, \quad F = \sqrt{\theta} (2 - \xi) + \tilde{F}. \quad (3.25)$$

From (3.17a) and (3.18) it is found that \tilde{G} and \tilde{F} satisfy the linearized equations

$$\sqrt{\theta} \left[\frac{\partial^2 \tilde{G}}{\partial \xi^2} - (2 - \xi) \frac{\partial^2 \tilde{F}}{\partial \xi^2} \right] = \theta^2 P' + \frac{1}{2} \theta' \quad (P = P(R)), \quad (3.26a)$$

$$\sqrt{\theta} \left[-\frac{\partial \tilde{F}}{\partial \xi} + \tilde{G} + (2 - \xi) \frac{\partial \tilde{G}}{\partial \xi} \right] = -\frac{1}{2} \theta, \quad (3.26b)$$

where the radial pressure gradient may now be significant. Differentiation of (3.26b) with respect to ξ and elimination of $\partial^2 \tilde{F}/\partial \xi^2$ from (3.26) yields

$$\sqrt{\theta} [1 - (2 - \xi)^2] \frac{\partial^2 \tilde{G}}{\partial \xi^2} = \theta^2 P' + \frac{1}{2} \theta'. \quad (3.27)$$

According to an argument similar to that below (3.21) the right hand side of (3.27) is necessarily zero at $\xi = 3$, implying that

$$P = 1/2\theta + \text{constant}, \quad (3.28)$$

and one can show from (3.26) that \tilde{G} and \tilde{F} are both linear functions of ξ .

In order to determine θ it is unnecessary to consider region II. Instead we continue the investigation of region I and seek a better approximation to the outer solution. Note first that the

[†] This identification is approximate: when higher order terms are considered we see that OB is located at $\xi = 3 + O(R^{-1})$ (see, for example, (6.5)).

term $\partial p/\partial\theta$ remains dominant in the θ -component of the equation of motion (3.7*b*), so that p is still just a function of R alone to lowest order. Second, since the flow defined by (3.13*b*) is irrotational, the dominant inertia term $-g\mathcal{D}g$ in (3.7*a*) is zero in its own right. It is therefore concluded that a magnetostatic balance is still achieved in which

$$f\mathcal{D}f = -p' + aa', \quad (3.29)$$

where the term aa' comes directly from the last term in (3.7*a*). The right hand side of (3.29) is zero, however, by (3.24), (3.28) and $P = p$. It is concluded, therefore, that f in the improved approximation is given by

$$f = -a \sin \theta + \tilde{f}, \quad (3.30)$$

where by (3.6) \tilde{f} satisfies the equation,

$$\frac{\partial^2 \tilde{f}}{\partial \theta^2} + \tilde{f} = 2a' \sin \theta. \quad (3.31)$$

The most general solution satisfying the boundary condition $\partial f/\partial\theta = 0$ at $\theta = \frac{1}{2}\pi$ is

$$\tilde{f} = -a'(\theta - \frac{1}{2}\pi) \cos \theta - \tilde{a} \sin \theta, \quad (3.32)$$

where \tilde{a} is, as yet, an undetermined function of R .

(*f*) Matching of inner and outer solutions

As $\theta \rightarrow 0$, f has the asymptotic form

$$f \rightarrow -(a + \tilde{a})\theta + \frac{1}{2}\pi a' \quad (3.33)$$

and matching with the corresponding inner solution, part of which is given by (3.22*b*), is achieved provided

$$\frac{1}{2}\pi a' = 2\sqrt{\Theta} = 2/a. \quad (3.34)$$

A solution of this equation is

$$a = \sqrt{(8R/\pi)}, \quad (3.35)$$

while the general solution contains an arbitrary constant which may be added to R . The constant may be absorbed, however, by R_0 in the definition (3.3) of R ! Finally we normalize the magnetic field \mathbf{b} so that $(a =) |\mathbf{b}| = M_1^{-\frac{1}{2}}$, when $r = M_1$ ($\sim l/L$) (see (2.2) and (2.13)). The condition implies that

$$R_0 = \pi/8M_1 - \ln M_1 \quad (\text{or} \quad \ln(\mathcal{L}/LM_1) = -\pi/8M_1). \quad (3.36)$$

(*g*) Summary

To the order of accuracy attempted in this section the solution in the inflow region I is

$$g = \sqrt{\left(\frac{\pi}{8R}\right)} \cos \theta + \frac{1}{2R} \sqrt{\left(\frac{\pi}{8R}\right)} (\theta - \frac{1}{2}\pi) \sin \theta, \quad (3.37a)$$

$$f = \sqrt{\left(\frac{8R}{\pi}\right)} \sin \theta - \sqrt{\left(\frac{2}{\pi R}\right)} (\theta - \frac{1}{2}\pi) \cos \theta, \quad (3.37b)$$

$$p = \frac{4R}{\pi}, \quad (3.37c)$$

where only the leading order coefficients of the trigonometric functions $\sin \theta$ and $\cos \theta$ have been retained (see (6.3) below). Here the dominant terms are determined by (3.13), (3.28) and

(3.35); the correction to f is given by (3.32) and the correction to g is readily derived from (3.8). Referred to rectangular cartesian coordinates x and y , the fluid velocity and magnetic field components are

$$u_x = -(4/\pi) M^{\frac{1}{2}}(\frac{1}{2}\pi - \theta), \quad u_y = -M^{\frac{1}{2}}, \quad (3.38a)$$

$$b_x = -M^{-\frac{1}{2}}, \quad b_y = -\frac{1}{2}M^{\frac{1}{2}}(\frac{1}{2}\pi - \theta), \quad (3.38b)$$

where

$$M = u_y/b_x = \pi/8R \quad (3.38c)$$

is the inflow Alfvén number which decreases with distance from the neutral point, O. The magnetic field is almost uniform and antiparallel to the x -axis, increasing in strength with distance from O. Since b_y is negative, the magnetic field lines are bowed inwards slightly towards the neutral point. By contrast the flow is again almost uniform but antiparallel to the y -axis, decreasing in strength with distance from O. The streamlines are, therefore, bowed as indicated in figure 1. The magnetic field is current-free (consequently force-free) and the flow is irrotational (but see § 6 below).

The inflow is separated from the outflow region II by the Alfvén line OA located approximately at

$$y = \Theta x \quad (\Theta = M). \quad (3.39)$$

Evidently this line is not straight but bends slightly with distance from O. In the outflow region II the total pressure is still

$$P = \frac{1}{2}M^{-1}, \quad (3.40)$$

as given by (3.37c), while u_x and b_y are given by (5.13) below. The values of u_y and b_x necessary to complete our picture are also given by (5.13) but are not determined by the results of this section. According to (5.13) the ratio u_y/u_x is very small of order M^2 implying that the streamlines are almost parallel to the x -axis, while b_y/b_x is positive and of order 1 implying that the magnetic field lines are bowed towards the neutral point as indicated in figure 1.

It is to be expected that our asymptotic solution is valid when

$$M \ll 1 \quad (\text{or } R \gg 1), \quad (3.41)$$

i.e. at distances from the origin large compared with the distance \mathcal{L} at which inertia and Lorentz forces in the inflow region are comparable. It transpires, however (see §§ 5–7 below) that there is a further region containing the Alfvén line OA (see figure 2), in which our approximations fail. Except for these regions, where the solution is undetermined, the model constructed in this section is almost unique. That is to say different values of \mathcal{L} lead to different solutions, but they are not independent. In fact, the whole family of solutions can be generated from a single solution just by a change of length scales (i.e. a similarity transformation). The uniqueness of our similarity solution, which stems from the analyticity condition at the first Alfvén line OB, should be contrasted with the wide range of similarity solutions proposed by Yeh & Axford (1970).

(h) *Petschek's solution*

Consider a region of finite size L_e large compared to \mathcal{L} . At distances from the neutral point of this order R takes the constant value

$$R_e = \ln(L_e/\mathcal{L}), \quad (3.42a)$$

and the inflow Alfvén number M_e is given by

$$R_e = \pi/8M_e = \pi/8M_1 + \ln(L_e/M_1L). \quad (3.42b)$$

On the length scale L_e , therefore, the Alfvén line OA is straight, while the magnetic field and flow in the inflow region I are to leading order uniform and of strengths

$$B_e = (M_1/M_e)^{\frac{1}{2}} B_1 \quad \text{and} \quad U_e = (M_e/M_1)^{\frac{1}{2}} U_1, \quad (3.43)$$

respectively.

Petschek (1964) developed a similar solution as a power series in M_1 on the basis that

$$M_1 \ll 1, \quad (3.44)$$

in direct contrast to our similarity solution valid at large R . Since he took no account of Alfvén line curvature, Petschek was obliged to terminate his Alfvén lines at a finite distance L_e in order for his expansion procedures to be consistent. In our model Alfvén line curvature between the central diffusion region and the distance L_e can be neglected provided $(M_1 - M_e)/M_1$ is small. This estimate puts a bound on L_e which by (3.42*b*) is

$$\ln(L_e/L) \ll \pi/8M_1. \quad (3.45)$$

At distances small compared with L_e our solution coincides with Petschek's and moreover the results (3.38)–(3.40) compare favourably with the refinements due to Vasyliunas (1975, equations (89), (30) and (44) respectively). Indeed as a result of these higher order approximations, Vasyliunas noticed the key similarity property of Petschek's solution which is fundamental to our similarity solution. In particular he noted that on any intermediate length scale lying between L and L_e , Petschek's solution could be formulated without explicit reference to either of the characteristic lengths L or L_e .

An inequality similar to (3.45) was derived by Petschek for the validity of his solution. In particular, he suggested that the solution would be valid until equality of the left hand side of (3.45) with $\pi/4M_1$ (see Petschek 1964, eqn. (30)) is achieved. The equality gives an estimate of the maximum possible value of the reconnection rate M_e (here almost the same as M_1), which provides a dimensionless measure of the approach velocity of merging magnetic field lines in a region of size L_e . By contrast, our solution is appropriate to an unbounded region and is in no way restricted by (3.45). Indeed rather than encountering difficulties at large distances the accuracy of the similarity solution not surprisingly improves, as $r^* \rightarrow \infty$. Nevertheless, since M decreases with distance from the neutral point, M_e is bounded above by M_1 . Moreover, as we see in §§ 8 and 9 below when the diffusion regions are investigated in detail the solutions can only be justified rigorously in Petschek's limit (3.44) of small M_1 . In this case R is large everywhere outside the central diffusion region (see (3.38*c*)) and takes the value R_e (see (3.42*b*)) at distance L_e from the neutral point. Here the solution (3.38) to (3.40) is valid except in the immediate vicinity of the Alfvén line OA. Further comparisons with Petschek's solution are made in § 10.

4. COMPLEX POTENTIALS FOR REGION I

In the previous section a first approximation to the flow and magnetic field far from the origin was obtained of extremely simple form (see § 3 (*g*)). There are, however, still some important details to be resolved. First, it is known that there are large concentrations of vorticity and electric current at the Alfvén line OA but how is it distributed elsewhere? Secondly, and related to the previous question, there is a non-uniform feature of the approximate solution in the vicinity of OA which is not apparent from the lowest order solution. To answer the question

and to resolve difficulties arising from the non-uniformities it is necessary to develop the approximate solutions to higher orders. In accomplishing this objective we gain confidence in the validity of the approximate solution described in § 3 (*g*) and a deeper understanding of the physical processes involved.

In the previous section a formal deductive approach was adopted in deriving the solution. The procedure not only demonstrated convincingly uniqueness of the solution for given M_1 but also emphasized the logical order in which the solution is developed. To some extent the formal approach is now abandoned and advantage is taken of the preliminary calculations of § 3 which indicate that the flow and magnetic field in region I are free of vorticity and electric current to a high order (see (3.37)). Consequently, the solution is decomposed into two parts; one potential, the other rotational, distinguished by the superscripts P and R respectively. The stream function ψ , magnetic potential χ and total pressure p are written as

$$\psi = \psi^P + \psi^R, \quad \chi = \chi^P + \chi^R, \quad p = p^P + p^R, \quad (4.1)$$

where

$$\nabla^2 \psi^P = \nabla^2 \chi^P = 0. \quad (4.2)$$

The potential part of the solution by itself automatically satisfies the equation of motion and gives rise to the total pressure

$$p^P = \frac{1}{2}(\mathbf{b}^{P2} - \mathbf{u}^{P2}) = \frac{1}{2}(\nabla \chi^P)^2 - \frac{1}{2}(\nabla \psi^P)^2. \quad (4.3)$$

There is, however, no reason to suppose that the frozen field equation can be satisfied by purely potential flows and magnetic fields. The resulting failure of the frozen field equation is measured by

$$\epsilon = 1 + (\mathbf{u}^P \times \mathbf{b}^P)_z. \quad (4.4)$$

The main objective of this section is to show how ψ^P and χ^P can be constructed to satisfy the boundary conditions

$$\psi^P = \partial \chi^P / \partial \theta = 0 \quad (\theta = \frac{1}{2}\pi), \quad (4.5a)$$

$$\psi^P = \chi^P = r h^P(R) \quad (\theta = \Theta(R)), \quad (4.5b)$$

where $h^P(R)$ is, as yet, an undetermined function, at the same time ensuring that ϵ is small by comparison with unity.

The problem posed above by (4.2), (4.4) and (4.5) is ideally suited to complex variable methods. Corresponding to the functional forms (3.2) we introduce

$$\psi^P = \text{Re} \{zw(Z)\}, \quad \chi^P = \text{Im} \{-zv(Z)\} \quad (4.6a)$$

so that the velocity and magnetic field have the complex representations

$$e^{-i\theta}(u_r^P - iu_\theta^P) = i(w + dw/dZ), \quad e^{-i\theta}(b_r^P - ib_\theta^P) = -(v + dv/dZ), \quad (4.6b)$$

where Re and Im denote the real and imaginary parts respectively,

$$z = x + iy = r e^{i\theta}, \quad (4.6c)$$

$$Z = R_0 + \ln(z/i) = R + i(\theta - \frac{1}{2}\pi). \quad (4.6d)$$

Accordingly (4.4) may be expressed compactly in the form

$$\epsilon = 1 - \text{Re} \{(w + dw/dZ) \overline{(v + dv/dZ)}\}, \quad (4.7)$$

where the bar denotes complex conjugate. Moreover, the symmetry conditions (4.5a) and further use of (4.6) yield the equations

$$\operatorname{Im} \{w(R)\} = \operatorname{Im} \{v(R) + (dv/dR)(R)\} = 0, \quad (4.8a)$$

implying that w and v are real functions.† The specification of the problem for w and v is completed by application of the boundary condition (4.5b) at the Alfvén line OA. From the definition (4.6) this means that the additional conditions

$$\operatorname{Re} \{e^{i\Theta} w[R + i(\Theta - \frac{1}{2}\pi)]\} = \operatorname{Im} \{-e^{i\Theta} v[R + i(\Theta - \frac{1}{2}\pi)]\} = h^P(R) \quad (4.9)$$

must be imposed on w and v . Henceforth, when unspecified, it will be understood that the functions w and v are being evaluated at $Z = R$. Moreover a prime will be used to signify differentiation with respect to R ; for example, v' is the real function

$$v' = [dv/dZ]_{Z=R}. \quad (4.8b)$$

So far no approximations have been made. However, since it is only the far field solution, $R \gg 1$, which is under consideration we now utilize the property that the ratio $(\theta - \frac{1}{2}\pi)/R$ is small. Consequently, $w(Z)$ (and similarly $v(Z)$) is represented approximately by the Taylor series

$$w(Z) = w + i(\theta - \frac{1}{2}\pi)w' - \frac{1}{2}(\theta - \frac{1}{2}\pi)^2 w'' - \frac{1}{6}i(\theta - \frac{1}{2}\pi)^3 w''' + \dots \quad (4.10)$$

If it is supposed that the real functions w and v satisfy the equation

$$1 = \operatorname{Re} [(w + dw/dZ) \overline{(v + dv/dZ)}]_{Z=R - \frac{1}{2}i\pi} \quad (4.11a)$$

$$= (w + w')(v + v') - \frac{1}{2}(\frac{1}{2}\pi)^2 (w''v - 2w'v' + wv'') + \dots, \quad (4.11b)$$

then ϵ , defined by (4.7), is

$$\epsilon = \frac{1}{2}[(\theta - \frac{1}{2}\pi)^2 - (\frac{1}{2}\pi)^2] (w''v - 2w'v' + wv'') + \dots \quad (4.12)$$

By (4.10) the product wv is order 1 and, since differentiations with respect to R effectively reduce the order by a factor R^{-1} , it is clear from (4.12) that

$$\epsilon = O(R^{-2}) \quad \text{when} \quad \theta = O(1). \quad (4.13)$$

Moreover, since Θ is order R^{-1} (see (3.38) and (3.39)), the magnitude of ϵ in the vicinity of the Alfvén lines where $\theta = O(\Theta)$ is even smaller;

$$\epsilon = O(R^{-3}) \quad \text{when} \quad \theta = O(R^{-1}). \quad (4.14)$$

Consequently, on satisfying (4.11), the frozen field equation is satisfied throughout region I to a high order of accuracy. The increased accuracy for small θ transpires to be especially useful in tackling the analyticity requirement on the full solution (4.1) at the Alfvén line OB.

In the remainder of this section we proceed to use (4.11b) and a Taylor series approximation to (4.9) to determine w , v and Θ in terms of h^P . Now it is known from results of the previous section, namely (3.22a), (3.38) and (3.39), that the first approximations to $h^P(R)$ and $\Theta(R)$ are

$$h^P(R) = \sqrt{(\pi/8R)}, \quad \Theta(R) = \pi/8R. \quad (4.15)$$

† This is not strictly correct. In fact, part of v may be complex and proportional to e^{-R} . Such a term would lead, however, in the definition (4.6a) of χ to an irrelevant arbitrary constant which for convenience is chosen to be zero.

Consequently the expansion of (4.9) analogous to (4.11 *b*) is

$$w + O(R^{-\frac{1}{2}}) = -v\Theta - (\Theta - \frac{1}{2}\pi)v' + O(R^{-\frac{1}{2}}) = h^P(R). \quad (4.16)$$

The error estimates follow directly from the expansion (4.10) and the orders of magnitude of h^P and Θ given by (4.15). The approximate representation (4.16) can be extended to include higher order terms without difficulty. Only the terms given explicitly in (4.16), however, are required in the subsequent analysis.

Once w and v are known the total pressure

$$p^P(R, \theta) = \frac{1}{2}\{|v + dv/dZ|^2 - |w + dw/dZ|^2\} \quad (4.17)$$

(see (4.3)) is readily calculated. By (4.16) v is evidently of order $R^{\frac{1}{2}}$ and w is of order $R^{-\frac{1}{2}}$ so that the magnetic contribution to the pressure p^P is larger than the kinetic contribution by a factor order R^2 . A Taylor series expansion of (4.17) at the Alfvén line OA indicates that

$$p^P(R, \theta) = \frac{1}{2}(v + v')^2 + O(R^{-1}). \quad (4.18)$$

To make further progress it is anticipated that, for large R , $h^P(R)$ can be represented by

$$R^{\frac{1}{2}} h^P(R) = h_0^P + R^{-1}(h_{11}^P \ln R + h_1^P) + O[R^{-2}(\ln R)^2]. \quad (4.19a)$$

The corresponding forms for w , v , Θ and $p^P(R, \Theta)$ are

$$R^{\frac{1}{2}} w(R) = w_0 + R^{-1}(w_{11} \ln R + w_1) + O[R^{-2}(\ln R)^2], \quad (4.19b)$$

$$R^{-\frac{1}{2}} v(R) = v_0 + R^{-1}(v_{11} \ln R + v_1) + O[R^{-2}(\ln R)^2], \quad (4.19c)$$

$$R \Theta(R) = \Theta_0 + R^{-1}(\Theta_{11} \ln R + \Theta_1) + O[R^{-2}(\ln R)^2], \quad (4.19d)$$

$$R^{-2} p^P(R, \Theta) = R^{-1} p_1^P + O[R^{-2}(\ln R)]. \quad (4.19e)$$

Substitution of (4.19) into (4.11 *b*) and (4.16) yields

$$1 = w_0 v_0 + R^{-1}\{(w_{11} v_0 + w_0 v_{11}) \ln R + (w_1 v_0 + w_0 v_1)\} + O[R^{-2}(\ln R)^2], \quad (4.20a)$$

$$\begin{aligned} & w_0 + R^{-1}\{w_{11} \ln R + w_1\} + O[R^{-2}(\ln R)^2] \\ &= -v_0(\Theta_0 - \frac{1}{4}\pi) - R^{-1}\{[v_{11}(\Theta_0 + \frac{1}{4}\pi) + v_0 \Theta_{11}] \ln R + v_1(\Theta_0 + \frac{1}{4}\pi) \\ &\quad + v_0(\Theta_1 + \frac{1}{2}\Theta_0) - \frac{1}{2}\pi v_{11}\} + O[R^{-2}(\ln R)^2] \\ &= h_0^P + R^{-1}\{h_{11}^P \ln R + h_1^P\} + O[R^{-2}(\ln R)^2] \end{aligned} \quad (4.20b)$$

respectively.

The zero order coefficients together with (4.15) agree with the results of § 3 and give

$$w_0 = h_0^P = \sqrt{(\pi/8)}, \quad v_0 = \sqrt{(8/\pi)}, \quad \Theta_0 = \pi/8. \quad (4.21)$$

Equating the coefficients of $R^{-1} \ln R$ yields, with the aid of (4.21), the results

$$w_{11} = h_{11}^P, \quad v_{11} = -(8/\pi) h_{11}^P, \quad \Theta_{11} = \sqrt{(\frac{1}{2}\pi)} h_{11}^P, \quad (4.22a)$$

for w_{11} , v_{11} and Θ_{11} in terms of h_{11}^P ; while the coefficients of R^{-1} yield

$$w_1 = h_1^P, \quad v_1 = -(8/\pi) h_1^P, \quad \Theta_1 = -(\pi/16) + \sqrt{(\frac{1}{2}\pi)} (h_1^P - 2h_{11}^P). \quad (4.22b)$$

The corresponding value of p^P , is, by (4.18),

$$p_1^P = \frac{1}{2}v_0^2 = 4/\pi. \quad (4.23)$$

It will transpire later that the potential solution (4.19) is an accurate representation of the complete solution in region I including the rotational part up to order R^{-2} . This includes the terms order $R^{-2}(\ln R)^2$ and $R^{-2}(\ln R)$ in (4.19) which have not been considered explicitly! Consequently it is possible in the next section to consider region II to the same order and hence determine the unknown coefficients defining $h^P(R)$. Though all results to this order could have been obtained easily without recourse to complex variable procedures some advantages are gained. In particular, the representation is compact and the method of continuation of the expansion procedures to higher orders is transparent. These remarks are particularly pertinent to (4.12) which gives the amount by which the potential solution fails to satisfy the frozen equation, namely

$$\epsilon = \frac{1}{2}[(\theta - \frac{1}{2}\pi)^2 - (\frac{1}{2}\pi)^2] R^{-2} + O(R^{-3} \ln R). \quad (4.24)$$

5. THE SOLUTION FOR REGION II

The boundary layer solution (3.22a) in region II is here extended to the next order and matched across the Alfvén line OA with the potential solution of § 4. The distinctive character of the solution in region II stems from the pressure distribution. In region I the total pressure adjusts itself in a manner which allows the fluid flow a smooth passage up to the Alfvén line OA. Since the total pressure is continuous everywhere, its value in the boundary layer is effectively applied at the Alfvén line OA. In the zero order approximation of § 3 the total pressure gradient is negligible. In the higher order approximation considered in this section, however, the flow and magnetic field display new features which result directly from this pressure gradient.

It is natural to extend the solutions for F and G in ascending powers of R^{-1} . This simple procedure proves inadequate because of a degeneracy which becomes apparent later in the section (see (5.8) below). As already anticipated in § 4 $\ln R$ terms must be introduced and hence a solution of the boundary layer equations (3.17), (3.18) is sought of the form

$$G(R, \xi) = R^{-\frac{1}{2}}G_0(\xi) + R^{-\frac{3}{2}}\{G_{11}(\xi) \ln R + G_1(\xi)\} + O[R^{-\frac{5}{2}}(\ln R)^2], \quad (5.1a)$$

$$F(R, \xi) = R^{-\frac{1}{2}}F_0(\xi) + R^{-\frac{3}{2}}\{F_{11}(\xi) \ln R + F_1(\xi)\} + O[R^{-\frac{5}{2}}(\ln R)^2], \quad (5.1b)$$

$$P(R, \xi) = RP_1 + O[\ln R]. \quad (5.1c)$$

From (3.22a), the zero order solution is

$$G_0 = \Theta_0^{\frac{1}{2}}\xi, \quad F_0 = \Theta_0^{\frac{1}{2}}, \quad (5.2a)$$

where from (4.21), $\Theta_0 = \frac{1}{8}\pi. \quad (5.2b)$

The terms of order $R^{-2} \ln R$ and R^{-2} in (3.17a), (3.18) yield the four equations

$$\xi \, d^2G_{11}/d\xi^2 - d^2F_{11}/d\xi^2 = 0, \quad (5.3a)$$

$$\xi \, d^2G_1/d\xi^2 - d^2F_1/d\xi^2 = (\frac{1}{2} + P_1\Theta_0)\Theta_0^{\frac{1}{2}}, \quad (5.3b)$$

$$\xi \, dF_{11}/d\xi - F_{11} - dG_{11}/d\xi = -\Theta_{11}/\Theta_0^{\frac{1}{2}}, \quad (5.4a)$$

$$\xi \, dF_1/d\xi - F_1 - dG_1/d\xi = -(\Theta_1 + \frac{1}{2}\Theta_0)/\Theta_0^{\frac{1}{2}}. \quad (5.4b)$$

They comprise two pairs of coupled equations subject to the three boundary conditions $G = dF/d\xi = 0$ at $\xi = 0$ and $F = G$ at $\xi = 1$ and have the unique solutions

$$G_{11} = \frac{1}{2}(\Theta_{11}/\Theta_0^{\frac{1}{2}})\xi, \quad F_{11} = \frac{1}{2}(\Theta_{11}/\Theta_0^{\frac{1}{2}}), \quad (5.5a)$$

$$\left. \begin{aligned} G_1 &= [(\frac{1}{2}\Theta_1 + \frac{1}{4}\Theta_0)/\Theta_0^{\frac{1}{2}}]\xi - (\frac{1}{2} + P_1\Theta_0)\Theta_0^{\frac{1}{2}}\mathcal{G}(\xi), \\ F_1 &= [(\frac{1}{2}\Theta_1 + \frac{1}{4}\Theta_0)/\Theta_0^{\frac{1}{2}}] - (\frac{1}{2} + P_1\Theta_0)\Theta_0^{\frac{1}{2}}\mathcal{F}(\xi), \end{aligned} \right\} \quad (5.5b)$$

where

$$\left. \begin{aligned} \mathcal{G}(\xi) &= -\left(\frac{1+\xi}{2}\right)\ln\left(\frac{1+\xi}{2}\right) + \left(\frac{1-\xi}{2}\right)\ln\left(\frac{1-\xi}{2}\right) + \frac{1}{2}\xi, \\ \mathcal{F}(\xi) &= \left(\frac{1+\xi}{2}\right)\ln\left(\frac{1+\xi}{2}\right) + \left(\frac{1-\xi}{2}\right)\ln\left(\frac{1-\xi}{2}\right) + \frac{1}{2}. \end{aligned} \right\} \quad (5.5c)$$

In particular, the value of G and F on the Alfvén line OA is

$$\begin{aligned} G(R, 1) &= F(R, 1), \\ &= R^{-\frac{1}{2}}\Theta_0^{\frac{1}{2}} + R^{-\frac{3}{2}}\left[\frac{1}{2}(\Theta_{11}/\Theta_0^{\frac{1}{2}})\ln R + \frac{1}{2}(\Theta_1 - P_1\Theta_0^2)/\Theta_0^{\frac{1}{2}}\right] + O[R^{-\frac{5}{2}}(\ln R)^2]. \end{aligned} \quad (5.6)$$

To the order of accuracy considered here, g and f in region I take the same value $h^P(R)$ on the Alfvén line OA. It follows from (5.6) and (4.19a) that there is a second relation between $h^P(R)$ and $\Theta(R)$ in addition to that given by (4.21) and (4.22), namely

$$h_0^P = \Theta_0^{\frac{1}{2}}, \quad h_{11}^P = \frac{1}{2}(\Theta_{11}/\Theta_0^{\frac{1}{2}}), \quad (5.7a, b)$$

$$h_1^P = \frac{1}{2}(\Theta_1 - P_1\Theta_0^2)/\Theta_0^{\frac{1}{2}}. \quad (5.7c)$$

The matching involved in (5.7a) has, of course, already been achieved in § 3. After substitution of (5.7c) into (4.22b), Θ_1 cancels out. Consequently Θ_1 can take any value (which we write in (5.11) below as $\frac{1}{8}\pi(\frac{1}{2} - \alpha)$ provided

$$h_{11}^P = -\frac{1}{4}\sqrt{(\pi/8)}\left(\frac{1}{2} + P_1\pi/8\right). \quad (5.8)$$

Otherwise there is no solution of the algebraic equations! Since continuity of total pressure across the Alfvén line OA implies that

$$P_1 = p_1^P = 4/\pi, \quad (5.9)$$

the right hand side of (5.8) is non-zero. Thus without the $\ln R$ terms in the series expansions (4.19) and (5.1), the condition (5.8) cannot be met. The reason that the simple $\ln R$ does not introduce further complications can be seen from (5.7b) where again degeneracy occurs. This time though, it is trivial in as much as (5.7b) and the last equation (4.22a) are identical.

From (5.8), (5.9) and (4.22a) we obtain

$$w_{11} = h_{11}^P = -\frac{1}{4}\sqrt{(\pi/8)}, \quad v_{11} = \frac{1}{4}\sqrt{(8/\pi)}, \quad \Theta_{11} = -\frac{1}{2}(\pi/8). \quad (5.10)$$

The corresponding results (4.22b) become on using (5.8) and (5.9)

$$w_1 = h_1^P = -\frac{1}{2}\alpha\sqrt{(\pi/8)}, \quad v_1 = \frac{1}{2}\alpha\sqrt{(8/\pi)}, \quad \Theta_1 = \left(\frac{1}{2} - \alpha\right)(\pi/8), \quad (5.11)$$

where the value of the constant α is arbitrary. The introduction of the arbitrary constant is no surprise and was anticipated earlier in § 3 by the constant of integration in (3.35). As before the constant α may be absorbed by the constant R_0 in the definition (3.3) of R . The degeneracy encountered above is thus accounted for and no further degeneracy of this type can occur in the expansion procedure.

The results of this section may be summarized by substituting (5.2), (5.9), (5.10) and (5.11) into (5.5). It gives

$$G = \sqrt{(\pi/8R)} \{ \xi + R^{-1} [-\frac{1}{4}\xi \ln R + \frac{1}{2}(1-\alpha)\xi - \mathcal{G}(\xi)] + O[R^{-2}(\ln R)^2] \}, \quad (5.12a)$$

$$F = \sqrt{(\pi/8R)} \{ 1 + R^{-1} [-\frac{1}{4} \ln R + \frac{1}{2}(1-\alpha) - \mathcal{F}(\xi)] + O[R^{-2}(\ln R)^2] \}, \quad (5.12b)$$

$$P = 4R/\pi + O(\ln R). \quad (5.12c)$$

The x and y components of the fluid velocity and magnetic field in the outflow region II can be calculated from (5.12) and expressed in a form similar to (3.38). They are

$$u_x = M^{-\frac{1}{2}} + O(M^{\frac{1}{2}} \ln M), \quad u_y = -\frac{4}{\pi} M^{\frac{3}{2}} \left[\ln \left(\frac{1+\xi}{1-\xi} \right) - \xi \right] + O(M^{\frac{5}{2}} \ln M), \quad (5.13a)$$

$$b_x = -\frac{4}{\pi} M^{\frac{1}{2}} \ln \left(\frac{1+\xi}{1-\xi} \right) + O(M^{\frac{3}{2}} \ln M), \quad b_y = -M^{\frac{1}{2}} + O(M^{\frac{3}{2}} \ln M), \quad (5.13b)$$

where M is defined by (3.38c). Owing to the singularity at $\xi = 1$, the solutions (5.13) cease to be valid when $\ln |1-\xi|$ is of order $\ln M$. This non-uniformity of the asymptotic expansion is discussed in detail in § 7.

6. THE ROTATIONAL SOLUTION FOR REGION I

One attraction of the decomposition in § 4 of the solution into potential and rotational parts is that the expansion of the potential part is uniformly valid throughout region I. This is not the case for the rotational part which requires an inner expansion valid when θ is order R^{-1} and an outer expansion valid when θ is order 1. This happy state of affairs transpires to be especially useful since the potential part dominates the full solution. A word of caution is called for, however, as the decomposition into potential and rotational parts is not unique. Indeed the dominant term defining the so called rotational part of the magnetic field is potential! The reason for the anomaly stems from the boundary condition (4.5b). Here the requirement that ψ^P and χ^P must be equal is *ad hoc*, since any differences in their values may be accommodated by the rotational part of the solution. As a result a potential part of χ^R is generated at a lower level than is strictly necessary. The criterion adopted to specify the rotational part of the solution is that it should stem directly from the vorticity and electric current and satisfy boundary conditions similar to (4.5).

The main objective of this section is so determine the dominant part of the vorticity and electric current in region I. At the same time we have the added bonus of understanding how the series approximation may be systematically extended to higher orders.

The first step towards our goal is to represent the potential solution of § 4 explicitly in terms of the outer variables R , θ and the inner variables R , ξ . The outer and inner solutions are then represented in the form

$$g = g^P + g^R, \quad f = f^P + f^R, \quad p = p^P + p^R, \quad (6.1a, b, c)$$

$$G = G^P + G^R, \quad F = F^P + F^R, \quad P = P^P + P^R. \quad (6.2a, b, c)$$

According to (4.6), (4.19), (4.21), (5.10) and (5.11), g^P and f^P have the outer expansions

$$\sqrt{(8/\pi)} g^P = R^{-\frac{1}{2}} \cos \theta + R^{-\frac{3}{2}} \{ -\frac{1}{4} \ln R \cos \theta - \frac{1}{2} \alpha \cos \theta + \frac{1}{2} (\theta - \frac{1}{2} \pi) \sin \theta \} + O[R^{-\frac{5}{2}} (\ln R)^2], \quad (6.3a)$$

$$\sqrt{(\pi/8)} f^P = -R^{\frac{1}{2}} \sin \theta - R^{-\frac{1}{2}} \{ \frac{1}{4} \ln R \sin \theta + \frac{1}{2} \alpha \sin \theta + \frac{1}{2} (\theta - \frac{1}{2} \pi) \cos \theta \} + O[R^{-\frac{3}{2}} (\ln R)^2]. \quad (6.3b)$$

Although the potential solution (4.19) only gives terms in the outer expansion of f^P to order $R^{-\frac{3}{2}}(\ln R)^2$, it is in fact sufficiently accurate to give terms in the inner solution up to order $R^{-\frac{5}{2}}(\ln R)^2$. The reason for this is simple, since the expansion of f^P when θ is order R^{-1} is given by the middle term of (4.16) with Θ replaced by θ , namely

$$f^P = -\{(\theta - \frac{1}{2}\pi) v' + \theta v\} + O(R^{-\frac{5}{2}}). \quad (6.4a)$$

Here the terms are given correct to order $R^{-\frac{5}{2}}(\ln R)^2$ by (4.19). The corresponding expression for g^P is just

$$g^P = w + O(R^{-\frac{5}{2}}), \quad (6.4b)$$

which is independent of θ . The inner expansions defining G^P and F^P are deduced by putting $\theta = \Theta(R) \xi$ in (6.4) and using the expression (4.19) for Θ , v and w . They are

$$\sqrt{(8/\pi)} G^P = R^{-\frac{1}{2}} - R^{-\frac{3}{2}}\{\frac{1}{4} \ln R + \frac{1}{2}\alpha\} + O[R^{-\frac{5}{2}}(\ln R)^2], \quad (6.5a)$$

$$\sqrt{(8/\pi)} F^P = R^{-\frac{1}{2}}(2 - \xi) - R^{-\frac{3}{2}}\{\frac{1}{4} \ln R(2 - \xi) + (\alpha - 1) + (1 - \frac{1}{2}\alpha) \xi\} + O[R^{-\frac{5}{2}}(\ln R)^2]. \quad (6.5b)$$

The failure of the potential solution is first apparent when ϵ is non-zero. Since this occurs when ϵ is order R^{-2} it is reasonable to suppose that the rotational solution is smaller than the potential solution by the same order of magnitude. An outer solution is therefore sought taking the form

$$g^R = R^{-\frac{5}{2}} g_2^R(\theta) + O[R^{-\frac{7}{2}} \ln R], \quad (6.6a)$$

$$f^R = R^{-\frac{3}{2}} f_2^R(\theta) + R^{-\frac{5}{2}} \{\ln R f_{13}^R(\theta) + f_3^R(\theta)\} + O[R^{-\frac{7}{2}} (\ln R)^2], \quad (6.6b)$$

together with an inner solution taking the form

$$G^R = R^{-\frac{5}{2}} G_2^R(\xi) + R^{-\frac{7}{2}} \{\ln R G_{13}^R(\xi) + G_3^R(\xi)\} + O[R^{-\frac{9}{2}} (\ln R)^2], \quad (6.7a)$$

$$F^R = R^{-\frac{5}{2}} F_2^R(\xi) + R^{-\frac{7}{2}} \{\ln R F_{13}^R(\xi) + F_3^R(\xi)\} + O[R^{-\frac{9}{2}} (\ln R)^2]. \quad (6.7b)$$

To the order of accuracy indicated in (6.6) and (6.7) all nonlinearities involving the rotational part of the solution alone can be neglected in the governing equations (3.7), (3.8), (3.17) and (3.18). All nonlinearities involving the potential part of the solution alone can also be ignored provided 1 and Θ on the right hand side of (3.8) and (3.18) are replaced by ϵ and $\Theta\epsilon$ respectively (see § 4). The only remaining terms to be considered are the direct nonlinear couplings between the potential and rotational terms.

As pointed out in § 3, the key for determining the rotational part of the solution uniquely lies in the analyticity condition on the inner solution at $\xi = 3$. For this reason the development of the solution is begun in the inner region. From (6.2c) and (3.17b) it is clear that

$$\partial P^R / \partial \xi = O(G^P G^R / R) = O(R^{-4}) \quad (6.8)$$

and consequently to the order of approximation considered,

$$P^R = \text{constant} + R^{-1}\{P_{13}^R \ln R + P_3^R\} + O[R^{-2}(\ln R)^2], \quad (6.9)$$

where P_{13}^R and P_3^R are independent of ξ . To obtain the order of accuracy required by (6.7), equation (3.17a) may be approximated by

$$\begin{aligned} G^P \frac{\partial^2 G^R}{\partial \xi^2} + \Theta \frac{\partial(G^P, (1/\Theta) \partial G^R / \partial \xi)}{\partial(R, \xi)} \\ = \Theta^2 \frac{\partial P^R}{\partial R} + F^P \frac{\partial^2 F^R}{\partial \xi^2} + \Theta \left[\frac{\partial(F^P, (1/\Theta) \partial F^R / \partial \xi)}{\partial(R, \xi)} + \frac{\partial(F^R, (1/\Theta) \partial F^P / \partial \xi)}{\partial(R, \xi)} \right] + O(R^{-5}). \end{aligned} \quad (6.10)$$

Here it has been noted from (6.5) that

$$\partial G^P / \partial \xi = O[R^{-\frac{3}{2}}(\ln R)^2], \quad \partial^2 F^P / \partial \xi^2 = O[R^{-\frac{3}{2}}(\ln R)^2]. \quad (6.11)$$

Similar approximations are made to (3.18), which utilize (4.4), giving

$$-G^P \frac{\partial F^R}{\partial \xi} - \frac{\partial F^P}{\partial \xi} G^R + F^P \frac{\partial G^R}{\partial \xi} - \frac{\partial(G^R, F^P)}{\partial(R, \xi)} - \frac{\partial(G^P, F^R)}{\partial(R, \xi)} = \epsilon \Theta + O(R^{-5}), \quad (6.12a)$$

$$\text{where by (4.24)} \quad \epsilon = -R^{-2\frac{1}{2}}\pi\Theta\xi + O(R^{-4} \ln R). \quad (6.12b)$$

Note that according to (4.10) and (4.11), the $O(R^{-3} \ln R)$ error term in (4.24) reduces by a factor R^{-1} in the inner region. The only boundary conditions imposed on the solution are that $G^R(R, \xi)$ and $F^R(R, \xi)$ match with the outer solution, as $\xi \rightarrow \infty$, and that

$$G^R(R, 1) = F^R(R, 1) = h^R(R), \quad (6.13a)$$

where $h^R(R)$ is as yet an undetermined function whose first few terms are of the form

$$h^R(R) = R^{-\frac{3}{2}}h_2^R + R^{-\frac{7}{2}}\{h_{13}^R \ln R + h_3^R\} + O[R^{-\frac{9}{2}}(\ln R)^2]. \quad (6.13b)$$

We now proceed to substitute the expansion (6.7) for G^R and F^R into (6.10) and (6.12). Correct to order R^{-4} they yield

$$d^2G_2^R/d\xi^2 - (2-\xi) d^2F_2^R/d\xi^2 = 0, \quad (6.14a)$$

$$-dF_2^R/d\xi + G_2^R + (2-\xi) dG_2^R/d\xi = 0. \quad (6.14b)$$

Matching with the outer solution imposes the condition that G_2^R is finite, as $\xi \rightarrow \infty$ (see (6.6a) and (6.23a), (6.37) below). The only solution of (6.14) which satisfies this condition together with (6.13) is

$$G_2^R = h_2^R, \quad F_2^R = h_2^R \xi. \quad (6.15)$$

Equations similar to (6.14) are obtained by considering the terms of order $R^{-4} \ln R$ in (6.10) and (6.12). They are

$$d^2G_{13}^R/d\xi^2 - (2-\xi) d^2F_{13}^R/d\xi^2 = -(\pi/8)^{\frac{3}{2}} P_{13}^R, \quad (6.16a)$$

$$-dF_{13}^R/d\xi + G_{13}^R + (2-\xi) dG_{13}^R/d\xi = 0. \quad (6.16b)$$

The additional pressure term in (6.16a) is dismissed by the condition of analyticity on the solution at $\xi = 3$. There is no boundedness condition on G_{13}^R , as $\xi \rightarrow \infty$, so that the general solution satisfying the boundary condition (6.13) is

$$P_{13}^R = 0, \quad G_{13}^R = h_{13}^R + A_{13}(\xi - 1), \quad F_{13}^R = h_{13}^R \xi + A_{13}(\xi - 1), \quad (6.17)$$

where the constant A_{13} is, as yet, undetermined.

The above procedure is repeated. This time the terms order R^{-4} in (6.10) and (6.12) are retained giving

$$d^2G_3^R/d\xi^2 - (2-\xi) d^2F_3^R/d\xi^2 = -(\pi/8)^{\frac{3}{2}} P_3^R - h_2^R, \quad (6.18a)$$

$$-dF_3^R/d\xi + G_3^R + (2-\xi) dG_3^R/d\xi = -4(\pi/8)^{\frac{3}{2}} \xi + h_2^R. \quad (6.18b)$$

Elimination of F_3^R from (6.18) yields

$$\{1 - (2-\xi)^2\} d^2G_3^R/d\xi^2 = -(\pi/8)^{\frac{3}{2}} P_3^R - h_2^R + 4(\pi/8)^{\frac{3}{2}} (2-\xi). \quad (6.19)$$

The solution is analytic at $\xi = 3$ provided

$$P_3^R = -(\pi/8)^{-\frac{3}{2}} h_2^R - \frac{1}{2}\pi. \quad (6.20)$$

For this value of P_3^R the general solution of (6.18) satisfying the boundary condition (6.13) is

$$G_3^R = 4(\pi/8)^{\frac{1}{2}} (\xi - 1) [\ln (\xi - 1) - \frac{3}{2}] + (\frac{1}{2}h_2^R + A_3) (\xi - 1) + h_3^R, \quad (6.21 a)$$

$$F_3^R = 4(\pi/8)^{\frac{1}{2}} (\xi - 1) [\ln (\xi - 1) - \frac{1}{2}] + (A_3 - \frac{1}{2}h_2^R) (\xi - 1) + h_3^R \xi, \quad (6.21 b)$$

where A_3 is, as yet, an undetermined constant.

To achieve matching G^R and F^R must be expanded on the basis of ξ large. From (6.7), (6.15), (6.17) and (6.21) we obtain

$$G^R = R^{-\frac{1}{2}}h_2^R + R^{-\frac{7}{2}}\{A_{13}\xi \ln R + 4(\pi/8)^{\frac{1}{2}}\xi(\ln \xi - \frac{3}{2}) + (\frac{1}{2}h_2^R + A_3)\xi\} \\ + O[R^{-\frac{7}{2}} \ln R] + O[R^{-\frac{9}{2}}\xi \ln R], \quad (6.22 a)$$

$$F^R = R^{-\frac{1}{2}}h_2^R \xi + R^{-\frac{7}{2}}\{(h_{13}^R + A_3)\xi \ln R + 4(\pi/8)^{\frac{1}{2}}\xi(\ln \xi - \frac{1}{2}) + (A_3 - \frac{1}{2}h_2^R + h_3^R)\xi\} \\ + O[R^{-\frac{7}{2}} \ln R] + O[R^{-\frac{9}{2}}\xi \ln R]. \quad (6.22 b)$$

In terms of the outer variables this provides the two conditions

$$g^R \rightarrow R^{-\frac{1}{2}}\{(8/\pi)[A_{13} + 4(\pi/8)^{\frac{1}{2}}]\theta \ln R + h_2^R + (8/\pi)[4(\pi/8)^{\frac{1}{2}}(\ln \theta + \ln(8/\pi) - \frac{3}{2}) + \frac{1}{2}h_2^R + A_3]\theta\} \\ + O[R^{-\frac{7}{2}} \ln R], \quad (6.23 a)$$

$$f^R \rightarrow R^{-\frac{1}{2}}(8/\pi)h_2^R \theta + R^{-\frac{7}{2}}\{(8/\pi)[h_{13}^R + A_{13} + 4(\pi/8)^{\frac{1}{2}}]\theta \ln R \\ + (8/\pi)[4(\pi/8)^{\frac{1}{2}}(\ln \theta + \ln(8/\pi) - \frac{1}{2}) + A_3 - \frac{1}{2}h_2^R + h_3^R]\theta\} + O[R^{-\frac{7}{2}} \ln R], \quad (6.23 b)$$

on the outer solution, as $\theta \rightarrow 0$. In view of the assumed form of g^R in (6.6a) the condition of the boundedness on G_2^R , as $\xi \rightarrow \infty$, is clearly correct. If the condition was not applied a term which behaves like $R^{-\frac{3}{2}}\theta$ would appear in (6.23a). Moreover, in order that no terms order $R^{-\frac{1}{2}} \ln R$ should appear in (6.6a), it is necessary that

$$A_{13} = -4(\pi/8)^{\frac{1}{2}}, \quad (6.24)$$

a condition which eliminates the leading term in (6.23a). No further information is gained without determining the solution (6.6) to the outer problem in detail.

To the order of accuracy required by (6.6b), equation (3.7) may be approximated by

$$0 = -\frac{\partial P^R}{\partial R} - f^P \mathcal{D} f^R - \frac{\partial(f^P, \partial f^R / \partial \theta)}{\partial(R, \theta)} - \frac{\partial(f^R, \partial f^P / \partial \theta)}{\partial(R, \theta)} + O(R^{-3}), \quad (6.25 a)$$

$$0 = -\frac{\partial P^R}{\partial \theta} + O(R^{-2}). \quad (6.25 b)$$

According to (6.25b), p^R is independent of θ to the order required by (6.25a) and is given by the inner solution (6.9) and (6.20). It is

$$p^R = \text{const} - \{(\pi/8)^{-\frac{3}{2}}h_2^R + \frac{1}{2}\pi\} R^{-1} + O[R^{-2} \ln R]. \quad (6.26)$$

Since the largest term in (6.25a) is $f^P \mathcal{D} f^R$, the magnetic field is current-free to lowest order. Hence the first two coefficients in the expansions (6.6b) for f^R which take account of the boundary condition (6.23b) are

$$f_2^R = (8/\pi)h_2^R \sin \theta, \quad (6.27)$$

$$f_{13}^R = (8/\pi)h_{13}^R \sin \theta, \quad (6.28)$$

where reduction to the latter result is achieved by (6.24). The value of f_3^R is now determined by equating the terms order R^{-2} in (6.25) which yield the equation

$$0 = -\frac{1}{2}\pi + \sqrt{(8/\pi)} \sin \theta \{d^2 f_3^R/d\theta^2 + f_3^R - (24/\pi)h_2^R \sin \theta\}. \quad (6.29)$$

The general solution satisfying the symmetry condition ($\partial f/\partial \theta = 0$) at $\theta = \frac{1}{2}\pi$ is

$$f_3^R = -4(\pi/8)^{\frac{3}{2}} \left\{ (\theta - \frac{1}{2}\pi) \cos \theta - \sin \theta \ln (\sin \theta) \right\} \\ - (12/\pi) h_2^R (\theta - \frac{1}{2}\pi) \cos \theta + D_3 \sin \theta, \quad (6.30)$$

where D_3 is, as yet, an undetermined constant. A match with (6.23 *b*) is achieved, as $\theta \rightarrow 0$, provided

$$h_2^R = -\frac{8}{3}(\pi/8)^{\frac{3}{2}} \quad (6.31a)$$

and

$$D_3 = 4(\pi/8)^{\frac{3}{2}} \left[\ln (8/\pi) - \frac{1}{6} \right] + (8/\pi) (A_3 + h_3^R). \quad (6.31b)$$

From (6.6 *b*), (6.30) and (3.6) the electric current in the outer region is given to a first approximation by

$$j = -\frac{4(\pi/8)^{\frac{3}{2}}}{rR^{\frac{3}{2}} \sin \phi} \left[\phi = \frac{\theta - \Theta}{\frac{1}{2}\pi - \Theta} \frac{1}{2}\pi \right]. \quad (6.32)$$

With the singularity located at $\theta = \Theta$, (6.32) is also valid in the inner region as can be seen from (6.7 *b*) and (6.21 *b*). Consequently (6.32) is a uniformly valid approximation throughout region I. In the same notation the electric current in region II determined from (5.5) is to lowest order

$$j = \frac{(\pi/8)^{\frac{3}{2}}}{rR^{\frac{3}{2}}(\Theta^2 - \theta^2)}. \quad (6.33)$$

Evidently, the electric current density in region II is larger than that in region I by a factor of order R^2 for the inner region ($\theta/\Theta = O(1)$) and by a factor of order R^3 for the outer region ($\theta = O(1)$).

Finally the frozen field equation (3.8) is considered to determine g_2^R . It may be written with the aid of (4.4) as

$$-g^R(\partial f^P/\partial \theta) - g^P(\partial f^R/\partial \theta) + f^P(\partial g^R/\partial \theta) + f^R(\partial g^P/\partial \theta) = \epsilon + O(R^{-4}). \quad (6.34)$$

With the aid of (6.3), (6.6), (6.27) and (4.24) this reduces to lowest order to

$$\sqrt{(8/\pi)} \left\{ -\sin \theta \, dg_2^R/d\theta + \cos \theta \, g_2^R - h_2^R \right\} = \frac{1}{2} \left\{ (\theta - \frac{1}{2}\pi)^2 - (\frac{1}{2}\pi)^2 \right\}. \quad (6.35)$$

The only solution satisfying the symmetry condition ($g = 0$) at $\theta = \frac{1}{2}\pi$ is

$$g_2^R = \frac{1}{2}(\pi/8)^{\frac{3}{2}} \left\{ [(\theta - \frac{1}{2}\pi)^2 - (\frac{1}{2}\pi)^2] \cos \theta - 2(\theta - \frac{1}{2}\pi) \sin \theta \ln (\sin \theta) \right. \\ \left. - 2 \sin \theta \int_0^{\frac{1}{2}\pi} \ln (\sin \theta') \, d\theta' \right\} - \frac{8}{3}(\pi/8)^{\frac{3}{2}} \cos \theta. \quad (6.36)$$

Matching with (6.23 *a*) is achieved provided

$$A_3 = (\pi/8)^{\frac{3}{2}} \left\{ \frac{10}{3} - 4 \ln (8/\pi) - (8/\pi) \int_0^{\frac{1}{2}\pi} \ln (\sin \theta') \, d\theta' \right\}. \quad (6.37)$$

At this stage the only independent undetermined constants are h_{13}^R and h_3^R and these are not fixed until higher order terms are considered.

Differentiation of (6.35) gives,

$$\frac{d^2 g_2^R}{d\theta^2} + g_2^R = -\sqrt{\left(\frac{\pi}{8}\right)} \frac{\theta - \frac{1}{2}\pi}{\sin \theta}. \quad (6.38)$$

Hence as in the case of the electric current a first approximation to the vorticity throughout region I is

$$\omega = \frac{(\pi/8)^{\frac{1}{2}} (\theta - \frac{1}{2}\pi)}{rR^{\frac{5}{2}} \sin \phi}. \quad (6.39)$$

Similarly the vorticity in region II derived from (5.5) is to lowest order

$$\omega = \frac{(\pi/8)^{-\frac{1}{2}} \theta}{rR^{\frac{1}{2}}(\theta^2 - \theta^2)}. \quad (6.40)$$

The main objective of the section is now achieved. In particular, the electric current and vorticity are known everywhere. Moreover the rôle of analyticity at the first Alfvén line OB and the process of iterating the approximate solution to higher orders are made clear. For example to improve the present results by order R^{-1} , it is necessary to derive the order $R^{-\frac{5}{2}}$ terms in (5.1). In the process $G(R, 1)$ defined by (5.6) is determined to the same order. The potential solution of § 4 can then be calculated to the higher order by application of the boundary condition

$$h^P(R) = G(R, 1) - h^R(R) \quad (6.41)$$

at the Alfvén line OA. The value of $h^R(R)$ is known to the required order of accuracy through the analysis of this section which determined h_2^R . This closes the problem for the flow in region II and the potential part of the solution in region I at the new order. At this stage the analysis of this section can be improved by order R^{-1} . The cycle outlined above can be continued indefinitely giving an asymptotic solution to any order required.

7. THE ALFVÉN LAYER

The solutions for the magnetic field and fluid velocity developed in §§ 5 and 6 are not uniformly valid asymptotic expansions as $\xi \rightarrow 1$. In particular the presence of terms proportional to $|1 - \xi| \ln |1 - \xi|$ in the expressions for F and G in (5.5) and (6.21) leads to field strengths and flow speeds which tend to infinity as $\xi \rightarrow 1$. Inspection of the order of magnitude of the terms in the series expansions (e.g. compare $\partial G_0/\partial \xi$ with $\partial G_1/\partial \xi$ defined by (5.2) and (5.5)) indicates that the breakdown occurs when

$$-\ln |1 - \xi| = O(\ln R). \quad (7.1)$$

The small region adjacent to the Alfvén line OA in which this order of magnitude relation holds will be called the Alfvén layer.

Perhaps the most straightforward procedure for determining the solution in the Alfvén layer is to introduce the characteristic velocities

$$\mathbf{v}_{\pm} = \mathbf{u} \pm \mathbf{b} \quad (7.2)$$

and consider the governing equations in characteristic form. The equation of motion and frozen field equation combine to yield the pair of coupled equations

$$(\mathbf{v}_- \cdot \nabla) \mathbf{v}_+ = -\nabla p, \quad (7.3a)$$

$$\frac{1}{2}(\mathbf{v}_- \times \mathbf{v}_+)_z = -1. \quad (7.3b)$$

The formal solution of (7.3 *a*) is

$$\mathbf{v}_+(\mathbf{x}) = \mathbf{v}_+(\mathbf{x}_0) - \int_{x_0}^x \frac{\nabla p}{|\mathbf{v}_-|} ds, \quad (7.4)$$

where the integration is along a C_- characteristic defined by

$$\psi_-(\mathbf{x}) = \psi_-(\mathbf{x}_0) = \text{constant} \quad (7.5 a)$$

and s measures distance along the characteristic. Here

$$\psi_{\pm} = \psi \pm \chi \quad (7.5 b)$$

is the stream function for a flow which has velocity \mathbf{v}_{\pm} and $\psi_- = 0$ defines the Alfvén line OA.

In both regions I and II the analyses of the previous sections have assumed continuity of both ψ and χ at the Alfvén line OA. The value taken by both ψ and χ on the line as given by (6.41) is

$$rh(R) = r[h^P(R) + h^R(R)] = rG(r, 1). \quad (7.6)$$

The assumption of continuity implies that the component of \mathbf{v}_+ normal to OA takes the same value on either side of the Alfvén layer. It is therefore reasonable to suppose that this component of \mathbf{v}_+ is almost constant across the layer and takes the value

$$2h \quad (7.7)$$

to lowest order. Since by hypothesis \mathbf{v}_- is almost parallel to OA in the Alfvén layer, equation (7.3 *b*) combined with the result (7.7) indicates that \mathbf{v}_- is also almost constant across the layer and takes the value

$$|\mathbf{v}_-| = 1/h \quad (7.8)$$

to lowest order. Again the total pressure p is assumed almost constant and so it follows that the only quantity which undergoes substantial variations across the layer is the component of \mathbf{v}_+ parallel to OA.

Within the framework of the above approximations the radial component of \mathbf{v}_+ can be computed directly from (7.4). Throughout the Alfvén layer the pressure given by (5.1 *c*) and (5.9) is

$$p = 4R/\pi + O(\ln R), \quad (7.9)$$

while h is calculated from (5.1 *a*) and (5.2) is

$$h = \sqrt{(\pi/8R)} + O(R^{-\frac{3}{2}} \ln R). \quad (7.10)$$

The corresponding value of ψ_- calculated directly from (7.8) and (7.10) is

$$\psi_- = -r\{\sqrt{(\pi/8R)}(1 - \xi) + O(R^{-\frac{3}{2}} \ln R)\}, \quad (7.11)$$

in agreement with the values determined from both (5.1) and (6.5) which are appropriate to the edge of the Alfvén layer. Since the C_- characteristics are almost radial lines, the element of length ds in (7.4) may be replaced by the element of radial distance dr and the magnitude of the component of \mathbf{v}_+ parallel to OA is given approximately by v_{+r} . With the aid of (7.9) and (7.10) the integration of (7.4) in the lowest order approximation is straightforward and yields

$$v_{+r} = -\sqrt{(8R/\pi)} + 2S(\psi_-) + O(R^{-\frac{1}{2}} \ln R), \quad (7.12)$$

where S is as yet an arbitrary function. Here the first term is forced by the pressure gradient and the second term is the constant of integration which takes different values on different C_- characteristics.

The inner expansions constructed in §§5 and 6 can now be utilized to determine the function S . Since equations (5.2), (5.5), (5.10) and (6.6) yield

$$\begin{aligned} v_{+r} &= \frac{1}{\Theta} \left(\frac{\partial F}{\partial \xi} + \frac{\partial G}{\partial \xi} \right) \\ &= \begin{cases} \sqrt{(8R/\pi)} \{1 + R^{-1}[\frac{1}{4} \ln R + \ln(1-\xi)] + O(R^{-1})\} & (\xi < 1), \\ -\sqrt{(8R/\pi)} \{1 + \frac{1}{4}R^{-1} \ln R + O(R^{-1})\} & (\xi > 1), \end{cases} \end{aligned} \quad (7.13)$$

matching is achieved when S is given by

$$S(\psi_-) = \begin{cases} \sqrt{\left(\frac{8R(|\psi_-|)}{\pi}\right)} & (\psi_- < 0), \\ 0 & (\psi_- > 0), \end{cases} \quad (7.14)$$

where $R(|\psi_-|)$ is the usual function R defined by (3.3) with the argument r replaced by $|\psi_-|$. Here terms order $R^{-\frac{1}{2}} \ln R$ and smaller have been neglected. Now when $-\ln|1-\xi|$ is of order $\ln R$,

$$S = \begin{cases} \sqrt{\left(\frac{8R}{\pi}\right)} \{1 + \frac{1}{2} \ln(1-\xi) + O(R^{-1} \ln R)\} & \text{in region II,} \\ 0 & \text{in region I} \end{cases} \quad (7.15)$$

and a clear match with (7.13) is obtained when $-\ln|1-\xi|$ is large compared with $\ln R$. Obviously higher order terms must be considered to obtain matching at the order $R^{-\frac{1}{2}} \ln R$ level when $-\ln(1-\xi)$ is of order $\ln R$.

It is evident from (7.13) that the singularity at $\xi = 1$ is still not removed. In fact on non-dissipative theory it cannot and reflects an inadequacy of our solution! The source of difficulty can be traced via the solution (7.4). In particular, suppose that \mathbf{x}_0 lies on the x or y axis. Then the integration can only be performed if ∇p and \mathbf{v}_- are known everywhere along the C_- characteristic passing through \mathbf{x}_0 . This will only be the case if $R(|\mathbf{x}_0|)$ is large. It follows that the solution (7.14) is invalid in the immediate vicinity of the Alfvén line OA but becomes valid at distances at which

$$R(|\psi_-|) \gg 1. \quad (7.16)$$

The two characteristic curves for which $R(|\psi_-|) = 1$ bound the shaded region in figure 2. A point to notice is that the two characteristics are almost parallel with the Alfvén line OA but slowly converge to it as $r \rightarrow \infty$. It is only well outside the region bounded by these two characteristics that our solution is valid.

Close to the Alfvén line OA, when ψ_- is small, $S(\psi_-)$ is undetermined. Elsewhere in the Alfvén layer, however, the radial flow velocities and magnetic field strengths are

$$u_r = S(\psi_-), \quad b_r = -\sqrt{\left(\frac{8R}{\pi}\right)} + S(\psi_-), \quad (7.17)$$

where $S(\psi_-)$ is given by (7.14). It is perhaps of some interest to note that these solutions provide us with the zeroth order approximation to the full solution throughout the extensive boundary layer structure, in which θ/Θ is order 1.

8. THE ALFVÉN BOUNDARY LAYERS AND CENTRAL DIFFUSION REGION

According to the equations governing the motion of an inviscid perfectly conducting fluid the tangential components of both magnetic field and fluid velocity may suffer discontinuities across an Alfvén line. The magnitude of the jump in value of the components is measured by the jump of $S(\psi_-)$ (see (7.12)) at $\psi_- = 0$. It is constant along the Alfvén line OA and measures the finite amount of electric current and vorticity concentrated on OA. For our problem, the situation is somewhat more complex inasmuch as $S(\psi_-)$ has a logarithmic singularity as $\psi_- \rightarrow 0$, which renders the solution undetermined before the value $\psi_- = 0$ is achieved. The singularity corresponds to large concentrations of electric current and vorticity similar to those noted by (6.32), (6.33), (6.39) and (6.40). In a fluid of finite viscosity and magnetic diffusivity neither sheets nor singular concentrations of electric current and vorticity can persist but, as time proceeds, must diffuse laterally. The subsequent diffusion may proceed in one of two ways. First, the layer may thicken indefinitely so that the concentrations of electric current and vorticity eventually disappear. Secondly, the tendency of the sheet to spread laterally may be overcome by convection at a characteristic velocity. In the former case there is no possibility of abrupt changes in the flow and magnetic field conditions in the final steady state. In the latter case, however, a steady state is possible in which the effects of diffusion are confined to a thin region which we call an Alfvén boundary layer. Outside the layer we may legitimately neglect dissipation. As in conventional boundary layer theory the influence of the finite size of the Alfvén boundary layer on the exterior non-dissipative solution is characterized by a small displacement thickness. This is, however, a high order effect with which we will not be concerned. Consequently, to determine the flow and magnetic field it is sufficient to impose the jump conditions described in §2 across the Alfvén line.

It cannot be overemphasized that the relevant convective velocity is not the fluid velocity \mathbf{u} but rather one of the characteristic velocities \mathbf{v}_+ or \mathbf{v}_- (see (7.2)). In particular, in the Alfvén layer OA convection along the layer results from the velocity \mathbf{v}_- . Here the solution is governed by the equations (7.3) modified to take account of dissipation. They are

$$(\mathbf{v}_- \cdot \nabla) \mathbf{v}_+ = -\nabla p + \nu_+ \nabla^2 \mathbf{v}_+ + \nu_- \nabla^2 \mathbf{v}_-, \quad (8.1a)$$

$$\frac{1}{2}(\mathbf{v}_- \times \mathbf{v}_+) + 1 = -\frac{1}{2}(M_1^{\frac{1}{2}} R_{m,1})^{-1} \nabla^2 (\psi_+ - \psi_-), \quad (8.1b)$$

where

$$\nu_{\pm} = \frac{1}{2} M_1^{-\frac{1}{2}} (R_{r,1}^{-1} \pm R_{m,1}^{-1}). \quad (8.1c)$$

In order to investigate the structure of the Alfvén boundary layer, we first confirm that the approximations and results (7.6)–(7.11) of the previous section remain valid. Within the framework of these approximations, the term $\nu_- \nabla^2 \mathbf{v}_-$ may be neglected in comparison with $\nu_+ \nabla^2 \mathbf{v}_+$. Thus as in §7 the component of \mathbf{v}_+ parallel to the layer is forced by the pressure gradient but now any singular behaviour is smoothed out by the diffusion term $\nu_+ \nabla^2 \mathbf{v}_+$. Since ∇p and $\nu_+ \nabla^2 \mathbf{v}_+$ are comparable, the term on the right of (8.1b) is small of order $|\nabla p| \delta (= O(R\delta))$, where $L\delta$ is the boundary layer thickness (see (8.7b) below). Consequently, in the first approximation at any rate we may neglect the term on the right of (8.1b) in comparison with unity and just investigate

$$(\mathbf{v}_- \cdot \nabla) \mathbf{v}_+ = -\nabla p + \nu_+ \nabla^2 \mathbf{v}_+ \quad (8.2)$$

in conjunction with (7.3b).

The C_- characteristics are almost straight lines and according to (7.11) are defined approximately by

$$\psi_- = \Theta^{-\frac{1}{2}}(\theta - \Theta) = \text{const.} \quad (8.3)$$

If we choose $X = \Theta^{\frac{1}{2}}\psi_{-}$, (8.4)

where LX measures distance normal to the Alfvén line OA, and r as our independent variables, then the radial component of \mathbf{v}_{+} is given approximately by the solution of

$$v_{-r} \frac{\partial}{\partial r} v_{+r} = -\frac{\partial p}{\partial r} + v_{+} \frac{\partial^2 v_{+r}}{\partial X^2}. \quad (8.5)$$

In the derivation of this equation from (8.2), we have ignored the curvature of the Alfvén line and neglected all terms which are smaller by an amount of order $R^{-1} \ln R$. Once the particular solution,

$$v_{+r} = -\sqrt{(8R/\pi)},$$

(see (7.12)) of (8.5), which is forced by the pressure gradient $\partial p/\partial r$, has been isolated, the remaining complementary function, which stems from the two remaining terms, has a simple physical interpretation. In (8.5), the term $v_{+} \partial^2 v_{+r}/\partial X^2$ describes the lateral diffusion of the passive scalar v_{+r} in an almost uniform stream \mathbf{v}_{-} , while the convection by this nearly parallel

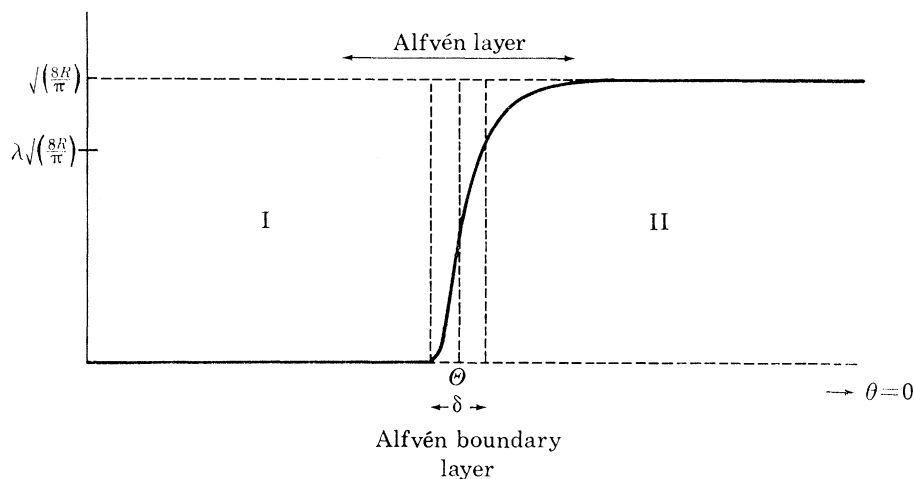


FIGURE 4. The radial velocity u_r in the neighbourhood of the Alfvén line $\theta = \Theta$ is plotted against the angle θ . The radial magnetic field b_r is $M^{-\frac{1}{2}} - u_r$. The thickness $L\delta$ of the Alfvén boundary layer is defined by (8.7b). In the case of negligible viscosity $\lambda = \{1 - \frac{1}{2}R^{-1} \ln R_m\}^{\frac{1}{2}}$, and $\lambda \rightarrow 1/\sqrt{2}$, as $r \rightarrow \infty$.

flow \mathbf{v}_{-} is approximated by the term $v_{-r} \partial v_{+r}/\partial r$. The solution of this diffusion problem which matches with the solution (7.12) in the non-dissipative part of the Alfvén layer when X is of the order δ (or equivalently when $\ln X$ equals $\ln \delta$) must satisfy the boundary conditions

$$v_{+r} \rightarrow \begin{cases} 0 & (X/\delta \rightarrow \infty), \\ 2S(-\delta/\Theta^{\frac{1}{2}}) & (X/\delta \rightarrow -\infty). \end{cases} \quad (8.6)$$

The similarity solution of this problem is well known and yields the solution

$$v_{+r} = -\sqrt{(8R/\pi)} + S(-\delta/\Theta^{\frac{1}{2}}) \{1 - \operatorname{erf}(X/\delta)\} \quad (8.7a)$$

of (8.5), where $\delta = \sqrt{(4v_{+r}/v_{-r})} = (4v_{+r})^{\frac{1}{2}}(\pi/8R)^{\frac{1}{4}}$. (8.7b)

Indeed, Alfvén boundary layers of this type have been investigated by a number of authors with application to flows past obstacles (see, for example, Dix (1963)). The value of the magnetic field and flow velocity defined throughout the Alfvén layer by (7.12) and (8.7) are illustrated graphically in figure 4 and a corresponding magnetic field line and streamline are sketched in

figure 5. Perhaps the most significant conclusion to be drawn from (8.7) is that diffusion is confined to a boundary layer of width $L\delta$, which increases with distance from the origin as $r^{\frac{1}{2}}$. The Alfvén boundary layer discussed here has its counterpart in the models of Yeh & Axford (1970) and Sonnerup (1970). The application of (8.5) to determine the Alfvén layer solutions corresponding to (7.12) and (8.7) for their models is described in Appendix B.

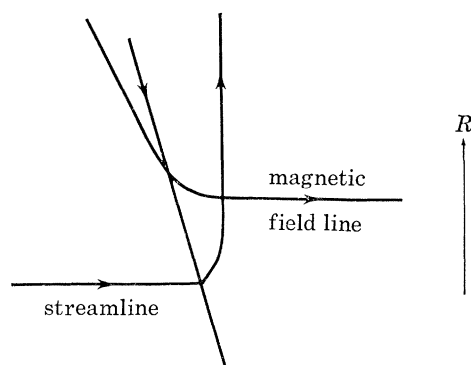


FIGURE 5. A typical streamline and magnetic field line in the vicinity of the Alfvén line OA are sketched. The radial distance has been suppressed by a log plot and hence $r(\theta - \Theta)$ and $\ln r$ measure distance normal and parallel to the layer respectively. Due to the compression the curvature of the streamline in region I and the magnetic field line in region II outside the Alfvén layer is not apparent.

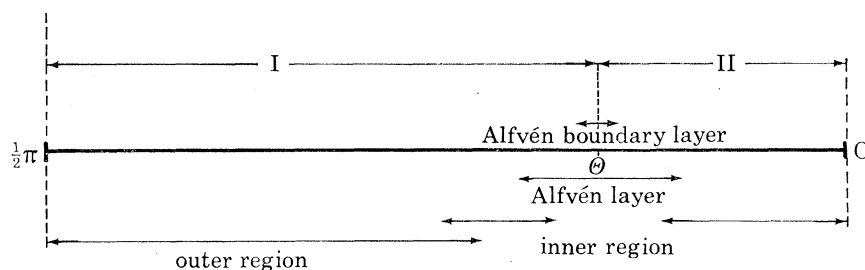


FIGURE 6. The various asymptotic regions, as $r \rightarrow \infty$, of the flow are summarized. The Alfvén line, $\theta = \Theta$, separates the inflow region I from the outflow region II. Boundary layer approximations are appropriate throughout the inner region, $\theta = O(\Theta)$, where Lorentz forces and inertia forces are comparable. Elsewhere in the outer region, $\theta = O(1)$, inertia forces are negligible. Part of the solution in region I is described by uniformly valid complex potentials. A small Alfvén layer is located in the neighbourhood of $\theta = \Theta$, which contains the³Alfvén boundary layer

The above analysis confirms that in the limit of zero dissipation the solution can accommodate discontinuities across the Alfvén line OA, and the various regions of the flow which we have isolated are summarized in figure 6. The question whether or not similar discontinuities can be maintained across the Alfvén line OB can now be answered easily. Upon modification of the above analysis, the equation appropriate to a possible diffusion layer at OB is still (8.5) but the plus and minus signs appearing as suffixes are all interchanged. Moreover the value of v_{-r} is

$$v_{-r} = -\sqrt{(8R/\pi)},$$

which is equal in magnitude but opposite in sign to the value of v_{+r} at OA. This minor modification has disastrous consequences, since it describes convection by an almost uniform stream towards the origin. The implication is, of course, that any boundary layer structure must

thicken as the origin is approached. It follows that the layer has finite width only if it is initiated at a finite distance from the origin as suggested by Sonnerup (1970). For our unbounded model and that of Yeh & Axford (1970), where the discontinuities and singular behaviour must be initiated at infinity, boundary layers of finite thickness cannot be supported. Consequently, in the limit of zero dissipation, discontinuities across the Alfvén line OB cannot be permitted. Vasylunas (1975) has arrived at the same conclusion via a different argument. By inspection of Yeh & Axford's (1970) equations governing the similarity functions f and g (the case $n = 0$ in (3.1)) when dissipative effects are included, he argues that a solution of the equations with the required topological properties is impossible. Since the key rôles of convection and diffusion are isolated in (8.5), the success and failure of layers at OA and OB respectively are rendered self-evident. Hence, though we could use Vasylunas' (1975) argument to show that a similarity solution of the modified form of (8.5) appropriate to OB is impossible, such a demonstration is unnecessary.

When viscosity is unimportant so that the ratio $R_{m,1}/R_{r,1}$ is small we may approximate $2\nu_+$ by $M_1^{-\frac{1}{2}}R_{m,1}^{-1}$. In this case the Alfvén boundary layer thickness $L\delta$ reduces to

$$L\delta = r^*(2/R_m)^{\frac{1}{2}}, \quad (8.8a)$$

where

$$R_m = r(M_1/M)^{\frac{1}{2}} R_{m,1} \quad (8.8b)$$

is the magnetic Reynolds number based on the length r^* and the Alfvén velocity at that distance (see (2.12) and (3.38)). At the ends of the diffusion region, where r is unity, the width of the Alfvén layer is of order $LR_{m,1}^{-\frac{1}{2}}$ which by (2.14) is also of order l . As distance from the origin increases, δ increases but the ratio $\delta/r\Theta$ of the thickness of the Alfvén boundary layer to the width of the outflow region II decreases. Since the analysis of this section is valid when $\delta \ll r\Theta$, we conclude that our solution in the neighbourhood of $\theta = \Theta$ is valid when $r \gg 1$. On the other hand the solution is only of use to us if $S(-\delta/\Theta^{\frac{1}{2}})$ is known! This will be the case as close to the origin as the edge of the central diffusion region only if

$$M_1 \ll 1. \quad (8.9)$$

Thus in the case when $M_1 \ll 1$, we have established that the solution of the Alfvén boundary layer developed in this section matches with the solution of the non-dissipative equations presented in the previous sections everywhere outside the central diffusion region. To solve our problem completely it only remains to determine the solution inside the central diffusion region which matches with the inflow conditions, as $y/M_1 \rightarrow \infty$, and the downstream conditions, as $x \rightarrow \infty$. In view of the fact that the layer splits into two Alfvén layers, as $x \rightarrow \infty$, it is not surprising that its structure on the order L length scale is extremely complicated. Though boundary layer approximations are appropriate, the ensuing non linear problem presents a sobering prospect for two reasons. First, the existence of two well-defined length scales L and l precludes the possibility of seeking similarity solutions. Secondly since the transverse structure of the layer is so complex a power series solution such as that considered by Priest & Cowley (1975) and Cowley (1975) is likely to have a small radius of convergence; probably no bigger than the central core, $r^* = O(l)$. Nevertheless the physical processes at work in the layer are readily understood in terms of the merging of the two Alfvén boundary layers which lie in the quadrants $(x > 0, y > 0)$ and $(x > 0, y < 0)$. Restricting attention to the Alfvén layer OA, we have seen above that, since the important convective velocity \mathbf{v}_- is known accurately at large x , the mathe-

mathematical problem for \mathbf{v}_+ is linear. As x decreases to unity the value of \mathbf{v}_- near the Alfvén line OA is no longer known since it is influenced by the presence of the second Alfvén layer (about OA', say) in the quadrant ($x > 0, y < 0$). The Alfvén layer near OA can no longer be investigated in isolation and the two Alfvén layers must be investigated simultaneously. Consequently, in the central diffusion region, which might be called more aptly a double Alfvén layer, a highly complex non-linear relation exists between \mathbf{v}_+ and \mathbf{v}_- .

According to the above description of the central diffusion region the convective effect of the characteristic velocities \mathbf{v}_+ and \mathbf{v}_- serves to confine the boundary layer against the competitive effect of lateral diffusion. One implication is that the propagation of damped Alfvén waves along the layer plays as important a rôle as fluid convection in determining the layer's structure. This well known property means, of course, that disturbances initiated at the origin propagate out along Alfvén lines even in the diffusion region. Now the solution in the layer evidently responds to the external conditions at the outer edge $y \gg M_1$ but contrary to one's intuition the region influenced by the layer is not the outflow region II, as $x \rightarrow \infty$. Instead, convection at the characteristic velocities \mathbf{v}_- and \mathbf{v}_+ channels the region in which diffusive effects are important (see figure 2) into the two distinct Alfvén layers OA and OA' and here lateral diffusion quickly eradicates the influence of the central diffusion region (see (8.5)). We therefore conclude that in the small M_1 limit the relation between the outflow region II and the inflow region I owes nothing to the form of the solution in the central diffusion region.

9. AN INTEGRAL CONSTRAINT

When M_1 is large, there is a region, size $\mathcal{L}(\gg l)$, near the origin O but outside the central diffusion region where dissipation is negligible. Here and for some distance out along the Alfvén layers the similarity solution developed in §§ 3–7 is inapplicable (see figure 2). Now the model developed in those sections only provides a solution of the governing equations at sufficiently large distances from O. Such a solution is not necessarily an approximation to any exact solution of the governing equations valid throughout all space. Put another way, we may regard our similarity solution as defining a set of boundary conditions at infinity and ask if any solution of the governing equations exists which satisfies these conditions, i.e. is the problem well posed? To some extent this difficult question is pertinent to all values of M_1 and can only be answered satisfactorily if asymptotic solutions are produced in all regions of the flow which match up with each other correctly. Even in the small M_1 limit we were unable to produce an approximate solution for the central diffusion region. Nevertheless the arguments of § 8 indicated convincingly that this region is passive inasmuch as a solution will exist there which satisfies the conditions applied at the edge of the diffusion region. The arguments are less forceful when M_1 is of order 1 and fail completely when M_1 is large for the reasons given above. We are left, therefore, with the intriguing question: is our asymptotic solution only valid at large r when M_1 is less than some upper bound or is it valid for all M_1 ? Whatever the answer, it is clear from (3.42*b*) that the important measure of the reconnection rate M_e for a large region size L_e is likely to be less than unity.

Attempts have been made by various authors to by-pass the direct determination of the solution near the origin O, through the construction of certain integral constraints which must be satisfied by the solution. Most of the constraints appear to yield little useful information. An integral of Ohm's law due to Sonnerup (1970) provides one exception. Consider the total

electric current $(B_1 L/\mu)I$ across the quarter disk, radius r^* , bounded by the lines $\theta = 0, \frac{1}{2}\pi$, where

$$I = \int_0^r \int_0^{\frac{1}{2}\pi} rj \, d\theta \, dr = \int_0^{\frac{1}{2}\pi} r b_\theta \, d\theta. \quad (9.1)$$

Integration of Ohm's law (2.10) with respect to θ followed by application of the symmetry condition (2.17 *b*) yields

$$(M_1^{\frac{1}{2}} R_{m,1})^{-1} \frac{dI}{dr} = \frac{1}{2}\pi r + \frac{dK}{dr}, \quad (9.2a)$$

where

$$K = \int_0^{\frac{1}{2}\pi} \psi \frac{\partial \chi}{\partial \theta} \, d\theta = - \int_0^{\frac{1}{2}\pi} \chi \frac{\partial \psi}{\partial \theta} \, d\theta. \quad (9.2b)$$

Further integration yields

$$(M_1^{\frac{1}{2}} R_{m,1})^{-1} I = \frac{1}{4}\pi r^2 + K \quad (9.3)$$

(cf. Sonnerup 1970, equations (29) and (33)). The significant feature of this result is that the constant of integration, which is zero, is determined by conditions at the origin ($I(0) = K(0) = 0$). It follows that the result provides us with an additional constraint on the full solution which was never explicitly imposed in the previous sections. On the other hand the similarity assumption (3.2) implies that I and K have the functional forms

$$I = i(R) r, \quad K = k(R) r^2. \quad (9.4)$$

Consequently the constant of integration only influences very small terms in the expansions of g, f and p of order $e^{-R} (\equiv 1/r)$ and these are outside the scope of our analysis. Correct to order r^2 at any rate our solution automatically satisfies (9.3).

Now within the framework of the approximations made so far the planes of symmetry though parallel to the x and y axes do not have to be coincident with them. For suppose the neutral point is located at the point $O'(x_N, y_N)$, then the only effect upon the solution at large r in changing the origin from O to O' is to modify the order r^{-1} correction terms, i.e. the exponentially small terms. Herein lies the true significance of the constraint (9.3) and we may illustrate it by reference to the Sonnerup (1970) and Yeh & Axford (1970) models. Consider the implications of Sonnerup's suggestion that the Alfvén lines OA, OB do not necessarily intersect at the neutral point O' . In the idealized case of perfect conductivity everywhere (r finite, $(M_1^{\frac{1}{2}} R_{m,1})^{-1} \rightarrow 0$), we must expect that in general the constraint (9.3) will not be satisfied. Rather we will find that

$$k = -\frac{1}{4}\pi + k_2/r^2, \quad (9.5)$$

where k_2 is a constant. There is, however, one set of solutions which automatically satisfies the condition

$$k_2 = 0, \quad (9.6)$$

namely the Yeh & Axford similarity form (3.1). Thus though all the Sonnerup solutions at large r are to leading order similarity (in particular, Yeh & Axford) type solutions, it is only the very small correction terms associated with the precise location of the origin which are influenced by the condition (9.6). Therefore we are led to conclude that the only models which satisfy (9.6) have the origin and the neutral point coincident. Physically this means that the size of the diffusion region goes to zero in the limit of perfect conductivity. If, however, there is a diffusion region of finite size having finite conductivity, Sonnerup's suggestion may be valid.

10. DISCUSSION

The validity of Petschek's (1964) model for fast magnetic field reconnection was put in doubt when the alternative models of Sonnerup (1970) and Yeh & Axford (1970) appeared. They contain two discontinuities in each quadrant and, being of self-similar form, are valid at large distances from the diffusion region. The object of the present paper has been to search for asymptotic solutions in a similar spirit to Yeh & Axford but containing, more realistically, only one discontinuity in each quadrant. We have produced a detailed analytic model for the fast magnetic field reconnection process which supports Petschek's qualitative picture (see §3 (*h*)) and which we regard as putting Petschek's mechanism on a firm mathematical foundation. The main differences are that in Petschek's case conditions are effectively constant in the inflow and outflow regions whereas in our model the magnetic field strength varies to lowest order as the square root of the logarithm of the distance from the origin; it increases with distance in the inflow region and decreases in the outflow region. Also the Alfvén lines curve away from the incoming flows.

Our asymptotic solution holds when the local Alfvén number, based on the velocity U and the Alfvén velocity $B/\sqrt{(\mu\rho)}$ in the inflow region I, is small, i.e.

$$M (\equiv U\sqrt{(\mu\rho)}/B) \ll 1. \quad (10.1)$$

Since M decreases with distance from the neutral point, the relation (10.1) is always satisfied provided

$$r^* \gg \mathcal{L}, \quad (10.2)$$

where \mathcal{L} is the distance at which M is unity. When $M_1 \ll 1$, the diffusion regions are relatively large and the solution is valid everywhere outside them (see figure 2). When $M_1 = O(1)$, the diffusion regions are relatively small and the solution only satisfies the governing equations far away from the central diffusion region. Because of the non-trivial question as to the relevant boundary conditions (see §9) it is not clear whether or not there exists a solution to the full m.h.d. equations which joins the asymptotic solution to the central diffusion region solution. Provided the joining can be accomplished, we believe that our model is self-consistent. The model is well established when M_1 is small but not rigorously established when M_1 is of order unity.

By contrast with our detailed calculations of the structure of the outflow region II (see §§ 3 and 5), Petschek (1964) assumed that the conditions there are uniform. Green & Sweet (1966) and Priest (1972), however, severely criticized Petschek's mechanism when they tried to take account of spatial variations. They assumed that the plasma speed in region II decreases as the square of the distance and found from the shock relations that the gas pressure also decreases. Then the necessary deceleration can be provided only by the Lorentz force which results from magnetic field lines bowed dramatically in the opposite direction to that indicated in figure 1*a*. This raised two doubts as to the validity of Petschek's mechanism. It is not clear that a matching to the central diffusion region is possible and also, if the outward bowing persists in the compressible case, the reversal of the tangential field component is possibly unphysical. For our model on the other hand, both the gas pressure and the flow speed increase but only logarithmically with distance in the outflow region. The presence of the term $d^2F_1/d\xi^2$ in the equation of motion (5.3*b*) indicates that the acceleration is provided by the Lorentz force which arises from a mild bowing in just the direction indicated by figure 1*a*. Therefore, the doubts about the validity of Petschek's mechanism, which were raised by Green & Sweet (1966) and Priest (1972),

do not arise in our model. Furthermore, because of the hyperbolic nature of the problem, it is not possible to find similarity solutions with the same type of variation along the discontinuities as was imposed by these authors.

For our model of the Petschek mechanism we can establish, in the limit

$$M_1 \ll 1, \quad (10.3)$$

a set of relations between $U_i, B_i, U_e, B_e, U_o, B_o, l$ and L , where the subscripts i and e denote the inflow values at $x^* = 0, y^* = LM_1$ and L_e , respectively, and the subscript o denotes the outflow values at $x^* = L, y^* = 0$. The width of the diffusion region is $l = O(LM_1)$; its length is L . The value of the local Alfvén number at a distance of order L from the neutral point is determined from (3.42) by dropping the subscript e . It yields

$$M/M_1 = 1 + O(M_1 \ln M_1). \quad (10.4)$$

Consequently when M_1 is small, M is approximately constant along the whole length of the central diffusion region. It follows immediately from (5.13) that

$$U_o = U_i/M_1, \quad B_o = M_1 B_i. \quad (10.5)$$

These identities together with (2.13), (2.14) and (3.43) give the order of magnitude relations

$$\left. \begin{aligned} lU_o &= LU_i, \\ U_i &= (l\mu\sigma)^{-1}, \\ U_o B_o &= U_i B_i = U_e B_e \end{aligned} \right\} \quad (10.6)$$

(see Priest & Cowley (1975)), while from (8.8*b*) we have the additional relation

$$R_{m,e}/R_{m,i} = (L_e/L)(M_1/M_e)^{\frac{1}{2}}, \quad (10.7)$$

where $R_{m,e} = L_e V_e \mu \sigma$ is the magnetic Reynolds number based on the external conditions and $V_e = B_e/\sqrt{\mu\rho}$ is the external Alfvén speed. This identity together with (2.12) and (3.42*b*) yields

$$\pi/(8M_e) = \pi/(8M_1) + \frac{1}{2} \ln (R_{m,e}^2 M_1 M_e). \quad (10.8)$$

For given external conditions (i.e. $R_{m,e}$ fixed), it is readily seen that the derivative dM_e/dM_1 calculated from (10.8) vanishes when $M_1 = \frac{1}{4}\pi$. Hence according to (10.8) the maximum possible value of M_e is the solution of

$$M_{e,\max} = \pi/(4 \ln (R_{m,e}^2 \pi M_{e,\max}/4)), \quad (10.9)$$

which occurs when $M_1 = \frac{1}{4}\pi$. Indeed for large $\ln R_{m,e}$ (a condition unlikely to hold very well in practice) we have

$$M_{e,\max} = \pi/(8 \ln R_{m,e}) \quad (\ln R_{m,e} \gg 1). \quad (10.10)$$

Though $M_1 = \frac{1}{4}\pi$ is less than unity we have violated the stronger condition (10.3) upon which the analysis is based. Nevertheless because of the importance of the maximum reconnection rate $M_{e,\max}$ in application to reconnection theory we feel justified in drawing some conclusions of a qualitative nature from (10.8) even when M_1 is of order 1. In particular, in the limit of large $R_{m,e}$, the estimate (10.10) of $M_{e,\max}$ is one half of the value given by Petschek (1964, equation (31)) and agrees with the modification of Petschek's result given by Vasylunas (1975, equation (47)).

Petschek's mechanism gives reconnection at a rate which depends largely on the speed with which some external agency forces magnetic field lines at a large distance to approach the

neutral point. As the inflow velocity U_1 increases so the width l and the length L of the diffusion region shrink in value. We may therefore speculate that there is an upper limit on M_1 of unity when the central diffusion region is roughly square ($L = l$). Such a cut off is to some extent arbitrary since we have no quantitative justification in proposing an exact numerical bound on M_1 . It is perhaps worth noting that when $M_1 > 1$ rather than degrading magnetic into kinetic energy at the Alfvén line the process is reversed. Nevertheless from figure 7 and equation (10.9), we are led to the remarkable conclusion that the maximum value of M_e is in no way related to the maximum allowed value of M_1 !

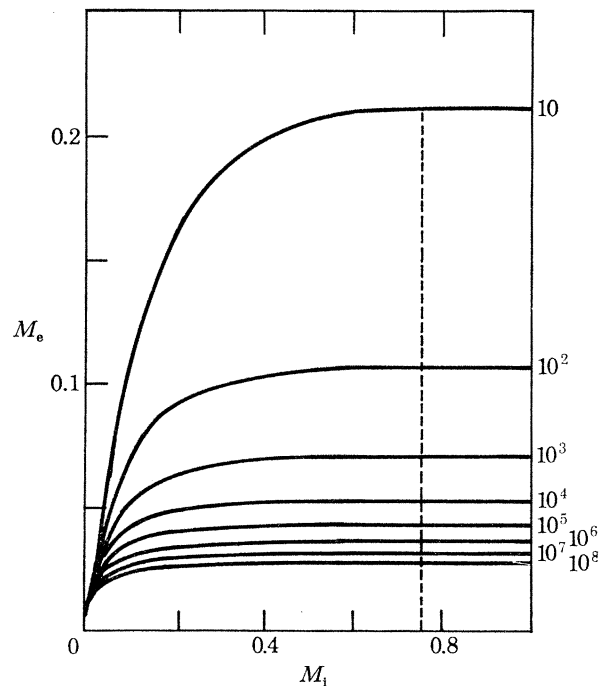


FIGURE 7. M_e is plotted against M_1 for various values of $R_{m,e}$ lying between 10 and 10^8 , according to (10.8). The maximum values of M_e , namely $M_{e,max}$, are located at the intersection of the curves with the broken line.

Suppose, as above, that M_1 must lie in the range 0–1. Evidently M_1 is not determined uniquely for values of M_e between $M_{e,max}$ and $M_{e,crit}$, which upon setting $M_1 = 1$ in (10.8) is determined by

$$M_{e,crit} = \{1 + (4/\pi) \ln (R_{m,e}^2 M_{e,crit})\}^{-1}. \quad (10.11)$$

As can be seen from figure 7 the values of $M_{e,crit}$ and $M_{e,max}$ are very similar. For instance, when $R_{m,e} = 10^8$, $M_{e,max} - M_{e,crit} = 0.001$. One can imagine a situation in which due to variations of the external conditions at large distances, M_e is increasing slowly in value. While M_e remains below $M_{e,crit}$, M_1 is uniquely determined but, as soon as M_e reaches $M_{e,crit}$, the possibility exists of M_1 jumping very quickly in value from $M_{1,crit}$ to unity. The result could be the explosive release of energy which several authors have claimed to be necessary for a solar flare trigger mechanism with the accompanying impulsive acceleration of particles (see, for example, Sweet 1969; Sturrock 1966). This suggestion should be regarded, however, as highly speculative, especially since figures 7 and 8 are strictly valid only when $M_1 \ll 1$.

The existence of a maximum reconnection rate $M_{e,max}$ confirms the results of Roberts & Priest (1975), who have recently constructed a model solution of Petschek's mechanism in a

finite region with the Alfvén line OA straight. They find the unique value of M_e for each value of the inclination α of OA. As α increases in value, so M_e passes through a maximum value which depends weakly on $R_{m,e}$. The maximum value decreases from 0.2 when $R_{m,e} = 10$ to 0.02 when $R_{m,e} = 10^6$. The present analysis complements the results of Roberts & Priest (1975) since it includes Alfvén line curvature and is valid at large distances. Moreover, it should be noted that in many applications $M_{e,\max}$ is possibly given by the condition that the smallest allowable value of l for the m.h.d. equations to be valid is the ion gyroradius (Sonnerup 1972).

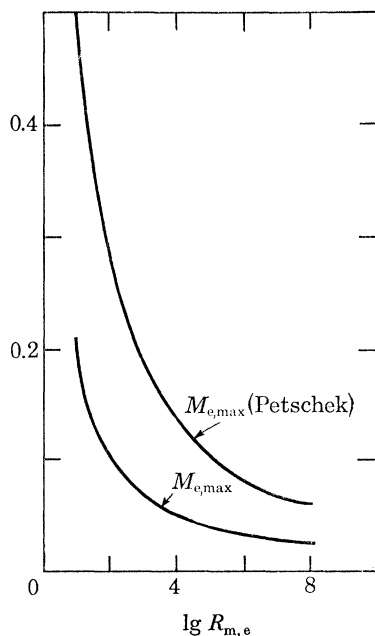


FIGURE 8. Our estimate (10.9) of $M_{e,\max}$ is plotted together with Petschek's estimate $M_{e,\max} = \pi/(4 \ln(M_{e,\max}^2 R_{m,e}))$ against $\lg R_{m,e}$.

Our final comment concerns Vasyliunas' (1975) recent review of the reconnection problem. He concludes, like us, that Petschek's mechanism does indeed work, but he considers a finite region rather than an unbounded one so that, unlike our analysis, effects of the boundary conditions are allowed to propagate inwards towards the diffusion region. His suggestion is that, with only one discontinuity in each quadrant, either a Petschek-like compression or a Sonnerup-like expansion may be present in the external region with the result that M_e may take any value, depending on the exact boundary conditions prescribed at the finite boundary. This may well be true but it begs the question as to what are the boundary conditions in a given application and, more important, it should be stressed that it is not necessarily possible to prescribe any values you like for the normal components of magnetic field and plasma velocity at the boundary. In our view, Vasyliunas' suggestion should therefore be regarded as speculative until it can be demonstrated rigorously.

The work described here was initiated while the authors were summer visitors at the National Center for Atmospheric Research, Boulder, Colorado, U.S.A. One of us (A.M.S.) attended the Advanced Study Program, the other (E.R.P.) the High Altitude Observatory with the help of a travel grant from the Carnegie Trust.

APPENDIX A

It was pointed out in §3 that the similarity forms

$$\psi = r^{1-n}g(\theta), \quad \chi = r^{1+n}f(\theta), \quad p = r^{2n}P(\theta) \quad (n > 0), \quad (\text{A } 1)$$

do not provide approximations to solutions of the reconnection problem. Arguments are put forward here to support this claim based solely on the condition that there is no discontinuity or singular behaviour permitted at the first Alfvén line OB.

According to (A 1) the ratio ψ/χ tends to zero, as $r \rightarrow \infty$, except on the line $\theta = \theta_0$ where $f(\theta_0) = 0$ (see figure 3). In this limit inertia is only important in a thin boundary-layer region adjacent to the line $\theta = \theta_0$ where the ratio χ/ψ is of order 1. It is here that the Alfvén lines OA and OB are located. Elsewhere the flow is slow and the magneto-static approximation

$$\nabla p = (\mathbf{b} \cdot \nabla) \mathbf{b} \quad (\text{A } 2)$$

and the frozen field equation $(\mathbf{u} \times \mathbf{b})_z = -1$ (A 3)

are appropriate. The θ -component of (A 2) together with (A 1) imply that P is independent of θ so that

$$P = \text{const.} \quad (\text{A } 4)$$

Upon taking the scalar product of (A 2) with \mathbf{b} we obtain the first integral

$$p - \frac{1}{2} \mathbf{b}^2 = \text{function of } \chi, \quad (\text{A } 5)$$

which states that the fluid pressure $p - \frac{1}{2} \mathbf{b}^2$ is constant on magnetic field lines. The similarity assumption (A 1) implies that the function appearing on the right of (A 5) must be proportional to $|\chi|^{2n/(1+n)}$. It follows that

$$P = \frac{1}{2} \{f'^2 + (n+1)^2 f^2\} + \beta |f|^{2n/(1+n)} \quad (f' = df/d\theta), \quad (\text{A } 6)$$

where β is an arbitrary constant.

Within the framework of the similarity assumption (A 1) the Alfvén line OA, where $\psi = \chi$, almost coincides with the line,

$$\theta = \theta_0 \quad (f(\theta_0) = 0) \quad (\text{A } 7)$$

for large r . In the inflow region I ($\theta_0 < \theta \leq \frac{1}{2}\pi$) f is negative and attains its minimum value $-a_I$ (say) at $\theta = \frac{1}{2}\pi$. Hence we set

$$f(\theta) = -a_I f_I(\theta) \quad (\text{A } 8)$$

so that by (A 6) f_I satisfies

$$f_I'^2 = (1+n)^2 (f_I^{2n/(1+n)} - f_I^2) + \lambda_I (1 - f_I^{2n/(1+n)}), \quad (\text{A } 9a)$$

where

$$\lambda_I = (1+n)^2 + 2\beta a_I^{-2/(1+n)}, \quad P = \frac{1}{2} \lambda_I a_I^2. \quad (\text{A } 9b)$$

There are three possible cases which are distinguished by λ_I being negative, zero or positive.

Case (i): $\lambda_I < 0$. The function f_I oscillates between 1 and a smaller positive constant, as θ increases. Since f_I is never zero a reconnection model is out of the question.

Case (ii): $\lambda_I = 0$. The solution (A 9) is

$$f_I = (\sin \theta)^{1+n}, \quad (\text{A } 10)$$

corresponding to the unidirectional magnetic field \mathbf{b} of strength

$$-(1+n) a_I y^n, \quad (\text{A } 11)$$

parallel to the negative x -axis. The stream function for the resulting fluid flow is determined from (A 3). It is

$$g_{\text{I}} = \frac{1}{(1+n)} \frac{\cos \theta}{a_{\text{I}} (\sin \theta)^n}. \quad (\text{A } 12)$$

Since θ_0 is zero, inertia is important only in a thin outflow region adjacent to the axis of symmetry, $\theta = 0$. Indeed according to (A 1), (A 8), (A 10) and (A 12) the inertia and Lorentz forces are comparable when

$$\theta = O(r^{-2n/(1+n)}). \quad (\text{A } 13)$$

The resulting boundary layer structure is investigated by stretching the θ coordinate and attempting the similarity solution

$$\psi = r^{\frac{1}{2}(1+m)} G(\xi), \quad \chi = r^{\frac{1}{2}(1+m)} F(\xi), \quad P = \frac{\alpha}{1-m} r^{1-m}, \quad (\text{A } 14a)$$

where

$$\xi = r^{1-m} \theta \quad (m = 1/(2n+1) < 1). \quad (\text{A } 14b)$$

Since $\lambda_{\text{I}} = 0$ implies that P is zero, the arbitrary constant α , which determines a relatively small pressure gradient in the boundary layer, is not determined by the first approximation (A 1) to the outer solution. Instead the value of α determined by the boundary layer solution imposes a boundary condition on the higher order approximations to the outer solution. On the other hand, the functions G and F , must satisfy the boundary conditions

$$G \rightarrow \frac{2m}{(1+m)} \frac{\xi^{-(1-m)/2m}}{a_{\text{I}}}, \quad F \rightarrow a_{\text{I}} \xi^{(1+m)/2m}, \quad \text{as } \xi \rightarrow \infty, \quad (\text{A } 15)$$

in order that a match can be achieved with the outer solution (A 10) and (A 12). Substitution of (A 14) into the radial component of the equation of motion (2.5a) and Ohm's law (2.10b) yields

$$\frac{1+m}{2} GG'' - \frac{1-m}{2} G'^2 = \frac{1+m}{2} FF'' - \frac{1-m}{2} F'^2 - \alpha, \quad (\text{A } 16a)$$

$$\frac{1+m}{2} (FG' - GF') = 1, \quad (\text{A } 16b)$$

upon neglect of dissipation. Differentiation of (A 16b) and elimination of G'' from (A 16a) yields

$$\frac{1+m}{2} (G^2 - F^2) F'' = F \left\{ \frac{1-m}{2} (G'^2 - F'^2) - \alpha \right\}. \quad (\text{A } 17)$$

The Alfvén lines OB and OA correspond to the points ξ_B and ξ_A at which F equals $-G$ and G respectively. The points ξ_B and ξ_A are singular points for the system of third order differential equations (A 16). The general solution of these equations possesses three arbitrary constants. By demanding that the solution is analytic at $\xi = \xi_B$, one constant is fixed and we find that the most general solution valid in the interval $\xi_A < \xi < \infty$, which contains ξ_B , is

$$G = -\sqrt{\left(\frac{\beta+\alpha}{1-m}\right)} (\xi+\alpha) + \frac{2}{1-m} \sqrt{\left(\frac{1-m}{\beta-\alpha}\right)}, \quad F = -\sqrt{\left(\frac{\beta-\alpha}{1-m}\right)} (\xi+\delta), \quad (\text{A } 18)$$

where β and δ are the remaining two arbitrary constants and the positive or negative square roots may be taken. A solution of this type cannot satisfy the boundary conditions (A 15), when $m < 1$, and so does not provide us with a solution of the reconnection problem. There appears

little doubt, however, that if the analyticity condition is not imposed at $\xi = \xi_B$, solutions can be obtained, similar in spirit to those of Yeh & Axford (1970).

The limit $m \rightarrow 1$ is of some interest. For if we let

$$\alpha + \beta = 0, \quad \alpha = -\frac{1}{2}(1-m) a_{\text{I}}^2, \quad (\text{A } 19)$$

equations (A 18) and (A 15) are compatible when $m = 1$! But the solution developed here is only valid for $m < 1$ and anyway the special case $m = 1$, investigated by Yeh & Axford (1970), also fails to satisfy the analyticity requirement. The result does, however, suggest that Yeh & Axford are close to the correct solution. It is for this reason that we attempt in this paper to modify their similarity solution ($n = 0$) by allowing g and f to vary slowly with respect to radial distance through their explicit dependence on $\ln r$ (see (3.2)) as well as θ .

Case (iii): $\lambda_{\text{I}} > 0$. From (A 9a), θ_0 may be determined. It is

$$\frac{1}{2}\pi - \theta_0 = \int_0^1 d\tau / \sqrt{[(1+n)^2(\tau^{2n(1+n)} - \tau^2) + \lambda_{\text{I}}(1 - \tau^{2n(1+n)})]} = I(\lambda_{\text{I}}) \quad (\text{A } 20a)$$

$$I(\lambda_{\text{I}}) < I(0) = \frac{1}{2}\pi. \quad (\text{A } 20b)$$

Hence θ_0 lies in the range 0 to $\frac{1}{2}\pi$ and only takes the value zero, when $\lambda_{\text{I}} = 0$. A solution similar to (A 8) is constructed in the outflow region II ($0 \leq \theta \leq \theta_0$). Here f is positive and attains its maximum value a_{II} (say) at $\theta = 0$. Therefore, we set

$$f(\theta) = a_{\text{II}} f_{\text{II}}(\theta), \quad (\text{A } 21)$$

where f_{II} is the solution of (A 9a) normalized by the condition

$$f_{\text{II}}(0) = 1. \quad (\text{A } 22)$$

All suffixes in (A 9) are replaced by II. The constants a_{II} and λ_{II} are not arbitrary but are determined by the two equations

$$I(\lambda_{\text{I}}) + I(\lambda_{\text{II}}) = \frac{1}{2}\pi, \quad P = \frac{1}{2}\lambda_{\text{II}} a_{\text{II}}^2. \quad (\text{A } 23)$$

The former condition ensures that θ_0 computed for regions I and II is the same. The latter condition ensures that the total pressure is continuous across the line $\theta = \theta_0$.

The flow in regions I and II is determined from the frozen field equation (A 3). Substitution of (A 1) yields

$$(1-n)gf' - (1+n)g'f = -1. \quad (\text{A } 24)$$

Once f is determined from (A 9), g can be determined from (A 24). The solution satisfying the boundary condition $\psi_r = 0$ at $\theta = 0$, $\frac{1}{2}\pi$ is

$$g(\theta) = \begin{cases} \frac{1}{(1+n) a_{\text{I}}} f_{\text{I}}^{(1-n)/(1+n)} \int_{\theta}^{\frac{1}{2}\pi} \frac{d\theta'}{[f_{\text{I}}(\theta')]^{2/(1+n)}} & (\theta_0 < \theta < \frac{1}{2}\pi), \\ \frac{1}{(1+n) a_{\text{II}}} f_{\text{II}}^{(1-n)/(1+n)} \int_0^{\theta} \frac{d\theta'}{[f_{\text{II}}(\theta')]^{2/(1+n)}} & (0 < \theta < \theta_0). \end{cases} \quad (\text{A } 25)$$

At $\theta = \theta_0$, (A 9) and (A 25) indicate that g and f' are continuous, provided $0 < n < 1$. In fact g and f are given by

$$g = \frac{1}{(1-n)\sqrt{(2P)}}, \quad f = -\sqrt{(2P)}(\theta - \theta_0) \quad (\text{A } 26)$$

to leading order in both regions I and II, when $|\theta - \theta_0|$ is small.

To lowest order at any rate the passage from region I to region II is smooth. A closer inspection of the higher order terms reveals difficulties. First a more accurate representation of f_I in the vicinity of θ_0 determined by (A 9a) is

$$f_I = \sqrt{(\lambda_I)} \phi + \frac{1}{2} \frac{1+n}{3n+1} \lambda_I^{(n-1)/(2(n+1))} [(1+n)^2 - \lambda_I] \phi^{(3n+1)/(n+1)} + \dots \quad (\phi > 0), \quad (\text{A } 27)$$

where $\phi = \theta - \theta_0$. Second the corresponding expansion for g is

$$g = \frac{1}{a_I \sqrt{(\lambda_I)} (1-n)} + O(\phi^q), \quad (\text{A } 28a)$$

where

$$q = \begin{cases} \frac{2n}{1+n} & (0 < n < \frac{1}{3}), \\ \frac{1-n}{1+n} & (\frac{1}{3} < n). \end{cases} \quad (\text{A } 28b)$$

Clearly, when n lies between 0 and 1, q lies between 0 and $\frac{1}{2}$. It follows that the radial velocity which is proportioned to g' tends to infinity, as $\phi \rightarrow 0$. Indeed when $n > 1$, g itself tends to infinity! For this reason attention is restricted to the less singular case $0 < n < 1$.

Evidently the neglect of inertia is unjustified in the immediate vicinity of $\theta = \theta_0$. Here inertia and Lorentz forces are comparable when ψ and χ are of the same size. Since this occurs when ϕ is order r^{-2n} , we attempt the boundary layer solution

$$\left. \begin{aligned} \psi &= \frac{r^{1-n}}{\sqrt{(2P)} (1-n)} + r^{1-n(1+2q)} G(\xi), \\ \chi &= -\sqrt{(2P)} r^{1-n} \xi + r^{1-n(1+2q)} F(\xi), \\ p &= Pr^{2n} + \frac{\alpha r^{2n(1-q)}}{2n(1-q)} \end{aligned} \right\} \quad (0 < n < 1, \xi = r^{2n}\phi). \quad (\text{A } 29)$$

Substitution of these expressions into the radial component of the equation of motion (2.5a) and Ohm's law (2.11) yields the pair of second order differential equations

$$(1/\sqrt{(2P)}) G'' = \sqrt{(2P)} \{2n(1-q) F' - (1-n) \xi F''\} - \alpha, \quad (\text{A } 30a)$$

$$(1/\sqrt{(2P)}) F' = \sqrt{(2P)} \{(1-n(1+2q)) G - (1-n) \xi G'\} \quad (\text{A } 30b)$$

(cf. the third order pair (A 16a, b)). As $\xi \rightarrow \infty$, the two complementary functions of (A 30) may be distinguished by the asymptotic laws

$$\left. \begin{aligned} G_1 &\sim \xi^{1-2nq/(1-n)}, & F_1 &\sim \xi^{-2nq/(1-n)}, \\ G_2 &\sim \xi^{2n(1-q)/(1-n)}, & F_2 &\sim \xi^{1+2n(1-q)/(1-n)}. \end{aligned} \right\} \quad (\text{A } 31)$$

Now when $n < \frac{1}{3}$, F_2 matches with (A 27), as $\xi \rightarrow \infty$ but G_1 becomes too large to match with (A 28): while when $\frac{1}{3} < n < 1$, G_2 matches with (A 28), as $\xi \rightarrow \infty$, but F_2 becomes too large to match with (A 27). Therefore, there is only one boundary layer solution which satisfies the matching conditions as $\xi \rightarrow \infty$. This unique solution does not satisfy the analyticity condition at $\xi = 1/[2P(1-n)]$, where the first approximations to ψ and $-\chi$ are equal. This further condition is only satisfied by a certain linear combination of G_1 and G_2 . The case $n = \frac{1}{3}$ requires special consideration but similar results follow. We must conclude that the boundary conditions on the boundary layer solution are too restrictive and that there is no solution to our problem

Of course, if non-analyticity is permitted at both Alfvén lines, solutions could be constructed as in case (ii) above.

The conclusion arrived at for case (iii) appears perfectly reasonable. Indeed one might anticipate that once inertia is significant, as it is near $\theta = \theta_0$, it would remain significant into the outflow region II. This is, however, contrary to the hypothesis that Lorentz forces dominate in both regions I and II. It is for this reason that case (ii) above in which region II collapses into the boundary layer is more attractive. It is unfortunate that case (ii) doesn't work either!

APPENDIX B

The two Alfvén lines OB and OA have their counterparts in the analyses of Yeh & Axford (1970) and Sonnerup (1970). In figure 5 of Yeh & Axford's paper they correspond to the straight lines 2' and 4' respectively in the top left quadrant. Our detailed analysis of the Alfvén layer in the neighbourhood of OA is directly applicable to the flow and magnetic field in the vicinity of 4'. Indeed the radial component of \mathbf{v}_+ is determined from (8.5) but (7.8)–(7.10) are replaced by

$$p = \alpha R, \quad v_{-r} = 1/h = \text{const} \quad (\theta = \text{const}), \quad (\text{B } 1)$$

where α is defined by Yeh & Axford (1970, equation (18a)). Outside the Alfvén boundary layer the solution corresponding to (7.11), (7.12) and (7.14) is

$$v_{+r} = -\alpha h R + 2S(\psi_-) \quad (= \alpha h \ln |\theta - \Theta|), \quad (\text{B } 2a)$$

where

$$\psi_- = -r(\Theta - \theta)/h, \quad (\text{B } 2b)$$

$$S(\psi_-) = \frac{1}{2}\alpha h \ln (h|\psi_-|), \quad (\text{B } 2c)$$

while inside the Alfvén boundary layer the solution corresponding to (8.7) is

$$v_{+r} = -\alpha h R + 2S(\delta/h) \quad (= \alpha h \ln (\delta/r)), \quad (\text{B } 3a)$$

where

$$\delta = \sqrt{4h v_{+r}}. \quad (\text{B } 3b)$$

Here (B 2a) describes the limiting behaviour of their solution, as $|\theta - \Theta| \rightarrow 0$. The Alfvén boundary layer solution (B 3) just indicates that the ever increasing value of $-v_{+r}$, as $\theta \rightarrow \Theta$, is cut off when dissipative effects become significant. The Sonnerup case $\alpha = 0$ is even simpler, since the term $-\alpha h R$ in (B 2a) is absent and the corresponding Alfvén boundary layer solution is

$$v_{+r} = \{S(0+) - S(0-)\} \text{erf}(X/\delta) + S(0+) + S(0-). \quad (\text{B } 4)$$

A similar jump occurs in Yeh & Axford's (1970) model but it is not apparent in the zero order solution (B 3).

Whereas the singular behaviour in the vicinity of the line 4' is acceptable, the singularity at the first Alfvén line 2' is not. The solution fails at the latter line for the reasons given in §8 for the Alfvén line OB. It is perhaps worth noting that the Alfvén layer solutions (B 2) and (B 3) for the Yeh & Axford (1970) model has some similarity with the Alfvén layer solutions (7.12) and (8.7). Our solution is, however, less singular in that v_{+r} does not vary significantly in size (it remains order $R^{1/2}$) and there is no reverse flow (cf. figure 4 and Yeh & Axford (1970), figure 5). In both cases the singular behaviour can be traced to the pressure gradient.

REFERENCES

- Cowley, S. W. H. 1975 *J. Plasma Phys.* **14**, 475.
 Dix, D. M. 1963 *J. Fluid Mech.* **15**, 449.
 Dungey, J. W. 1953 *Phil. Mag.* **44**, 725.
 Dungey, J. W. 1958 *Cosmic electrodynamics*. Cambridge University Press.
 Green, R. M. & Sweet, P. A. 1966 *Astrophys. J.* **147**, 1153.
 Hughes, W. F. & Young, F. J. 1966 *The electromagnetics of fluids*. New York: John Wiley & Sons, Inc.
 Parker, E. N. 1963 *Astrophys. J. Suppl. Ser.* **77**, **8**, 177.
 Parker, E. N. 1973*a* *J. Plasma Phys.* **9**, 49.
 Parker, E. N. 1973*b* *Astrophys. J.* **180**, 247.
 Petschek, H. E. 1964 AAS-NASA Symposium on the Physics of Solar Flares (ed. by W. N. Hess), NASA SP-50, 425.
 Petschek, H. E. & Thorne, R. M. 1967 *Astrophys. J.* **147**, 1157.
 Priest, E. R. 1972 *Mon. Not. R. astron. Soc.* **159**, 389.
 Priest, E. R. 1973 *Astrophys. J.* **181**, 227.
 Priest, E. R. & Cowley, S. W. H. 1975 *J. Plasma Phys.* **14**, 271.
 Priest, E. R. & Sonnerup, B. U. Ö. 1975 *Geophys. J. R. astron. Soc.* **41**, 405.
 Priest, E. R. & Soward, A. M. 1976 Proc. 71st IAU Symp. 'Basic mechanisms of solar activity'.
 Roberts, B. & Priest, E. R. 1975 *J. Plasma Phys.* **14**, 417.
 Roberts, P. H. 1967 *An introduction to magnetohydrodynamics*. London: Longmans, Green & Co. Ltd.
 Sonnerup, B. U. Ö. 1970 *J. Plasma Phys.* **4**, 161.
 Sonnerup, B. U. Ö. 1972 *NASA Symp. on High Energy Phenomena on the Sun*, Greenbelt, Maryland.
 Sturrock, P. 1966 *Nature, Lond.* **211**, 695.
 Sweet, P. A. 1958*a* Proc. of IAU Symp. on Electromagnetic Phenomena in Cosmical Physics (ed. B. Lehnert), p. 123. Cambridge University Press.
 Sweet, P. A. 1958*b* *Nuovo Cimento*, Suppl, **8**, ser. x, p. 188.
 Sweet, P. A. 1969 *Ann. Rev. Astr. Ap.* **7**, 149.
 Vasyliunas, V. 1975 *Rev. Geophys. Space Phys.* **13**, 303.
 Yeh, T. & Axford, W. I. 1970 *J. Plasma Phys.* **4**, 207.